Supporting Information

Engineering lanthanide-optical centres in IRMOF-3 by post-synthetic modification

Reda M. Abdelhameed,[a,b] Luis D. Carlos,[c] Artur M. S. Silva,*[b] and João Rocha*[a]

[a]Department of Chemistry, CICECO, University of Aveiro, 3810-193 Aveiro, Portugal.
[b]Department of Chemistry, QOPNA, University of Aveiro, 3810-193 Aveiro, Portugal.
[c]Department of Physics, CICECO, University of Aveiro, 3810-193 Aveiro, Portugal.

Table of contents

1. Elemental analysis

Table S1. Elemental analysis of IRMOF-3-CA, Ln-IRMOF-3-CA, IRMOF-3-GL and Ln-IRMOF-3-GL (Ln = Nd, Eu) (%).

Sample	Metal & chloride ratio *				C	H	N
	Zn	Nd	Eu	Cl			
IRMOF-3-CA $Zn_4C_{48}H_{51}N_5O_{19}$ = $[Zn_4O(C_{10}H_7NO_6)_3.2(C_2H_5)_3N]$	100	-	-	-	45.75 (45.63)	4.12 (4.07)	5.51 (5.54)
Nd-IRMOF-3-CA $Zn_4C_{30}H_{51}Cl_3Nd_3N_3O_{40}$ = $[Zn_4O(C_{10}H_{17}NO_{12}NdCl)_3]$	39.44 ±1.61	30.10 ±2.52	-	30.46 ±1.91	18.91 (19.02)	2.89 (2.71)	2.36 (2.22)
Eu-IRMOF-3-CA $Zn_4C_{30}H_{51}Cl_3Eu_3N_3O_{40}$ = $[Zn_4O(C_{10}H_{17}NO_{12}EuCl)_3]$	41.17 ±1.79	-	29.91 ±2.11	28.92 ±2.31	19.01 (18.79)	2.98 (2.68)	2.51 (2.19)
IRMOF-3-GL $Zn_4C_{28.5}H_{19.5}N_3O_{19.75}$ = $[Zn_4O(C_{10}H_7NO_7)_{2.25}(C_8H_5NO_4)_{0.75}]$	100	-	-	-	35.12 (34.88)	2.21 (2.00)	4.42 (4.28)
IRMOF-3-GL-R $Zn_4C_{28.5}H_{19.5}N_3O_{17.5}$ = $[Zn_4O(C_{10}H_7NO_6)_{2.25}(C_8H_5NO_4)_{0.75}]$	100	-	-	-	36.52 (36.20)	2.11 (2.08)	4.46 (4.44)
Nd-IRMOF-3-GL $Zn_4C_{55.5}H_{55.5}Cl_{2.25}N_{16.5}Nd_{2.25}O_{190.75}$ = $[Zn_4O(C_{22}H_{23}N_7O_7NdCl)_{2.25}(C_8H_5NO_4)_{0.75}]$	47.03 ±2.19	26.47 ±1.66	-	26.50 ±2.35	34.56 (34.44)	2.92 (2.89)	12.01 (11.94)
Eu-IRMOF-3-GL $Zn_4C_{55.5}H_{55.5}Cl_{2.25}Eu_{2.25}N_{16.5}O_{19.75}$= $[Zn_4O(C_{22}H_{23}N_7O_7EuCl)_{2.25}(C_8H_5NO_4)_{0.75}]$	47.53 ±3.15	-	26.20 ±1.66	26.27 ±1.05	34.20 (34.13)	2.91 (2.86)	11.88 (11.83)

*the percentage calculated from ICP analysis (repeated 3 times) and EDS and the results are expressed as mean ±SD for determination of 10 crystals. C, H, N percentages were measured for 3 samples and calculated value between brackets.

Table S2. Elemental analysis of IRMOF-3-EM, IRMOF-3-MVK, Ln-IRMOF-3-EM and Ln-IRMOF-3-MVK (Ln = Nd, Eu) (%).

Sample	Metal & chloride ratio*				S	C	H	N
	Zn	Nd	Eu	Cl				
IRMOF-3-EM $Zn_4C_{43.2}H_{39}N_3O_{22.6}$ = $[Zn_4O(C_{16}H_{15}NO_8)_{2.4}(C_8H_5NO_4)_{0.6}]$	100	-	-	-	-	43.01 (42.42)	3.32 (3.21)	3.51 (3.43)
Nd-IRMOF-3-EM $Zn_4C_{62.4}H_{96.6}Cl_{7.2}N_3Nd_{2.4}O_{32.2}S_{9\cdot6}$= $[Zn_4O(C_{24}H_{39}NO_{12}S_4NdCl_3)_{2.4}(C_8H_5NO_4)_{0.6}]$	29.44 ±2.35	17.64 ±1.12	- -	52.92 ±4.55	12.02 (11.96)	29.30 (29.11)	3.81 (3.78)	1.59 (1.63)
Eu-IRMOF-3-EM $Zn_4C_{62.4}H_{96.6}Cl_{7.2}N_3Eu_{2.4}O_{32.2}S_{9\cdot6}$= $[Zn_4O(C_{24}H_{39}NO_{12}S_4EuCl_3)_{2.4}(C_8H_5NO_4)_{0.6}]$	28.99 ±3.55	-	17.99 ±1.13	53.02 ±4.15	11.89 (11.87)	29.02 (28.90)	3.72 (3.75)	1.65 (1.62)
IRMOF-3-MVK $Zn_4C_{33.12}H_{28.68}N_3O_{15.28}$ = $[Zn_4O(C_{12}H_{11}NO_5)_{1.38}(C_{12}H_{11}NO_5)_{0.9}(C_8H_5NO_4)_{0.72}]$	100	-	-	-	-	41.62 (40.81)	3.05 (2.97)	4.09 (4.31)
Nd-IRMOF-3-MVK $Zn_4C_{55.92}H_{94.8}C_{l4.56}N_3Nd_{2.28}O_{26.68}S_{11.4}$= $[Zn_4O(C_{22}H_{40}NS_5O_{10}NdCl_2)_{1.38}(C_{22}H_{40}NS_5O_{10}NdCl_2)_{0.9}(C_8H_5NO_4)_{0.72}]$	36.88 ±3.21	21.08 ±1.18	-	42.04 ±2.05	15.65 (15.53)	28.66 (28.54)	4.12 (4.06)	1.82 (1.79)
Eu-IRMOF-3-MVK $Zn_4C_{55.92}H_{94.8}C_{l4.56}Eu_{2.28}N_3O_{26.68}S_{11.4}$ = $[Zn_4O(C_{22}H_{40}NS_5O_{10}EuCl_2)_{1.38}(C_{22}H_{40}NS_5O_{10}EuCl_2)_{0.9}(C_8H_5NO_4)_{0.72}]$	37.05 ±3.19	-	19.93 ±1.10	43.02 ±2.19	15.31 (15.42)	28.44 (28.32)	4.09 (4.03)	1.81 (1.77)

*the percentage calculated from ICP analysis (repeated 3 times) and EDS and the results are expressed as mean ±SD for determination of 10 crystals. C, H, N percentages were measured for 3 samples and calculated value between brackets.

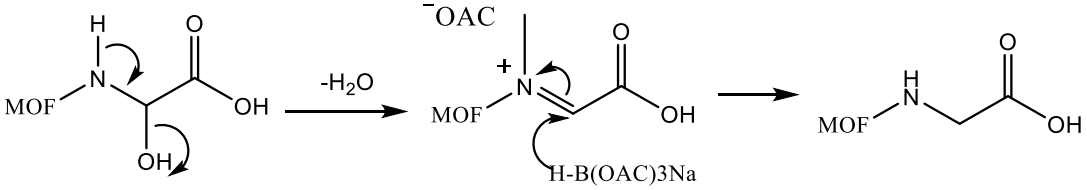

Scheme S1. Reductive amination mechanism using sodium triacetoxyborohydride

2. X-Ray diffraction

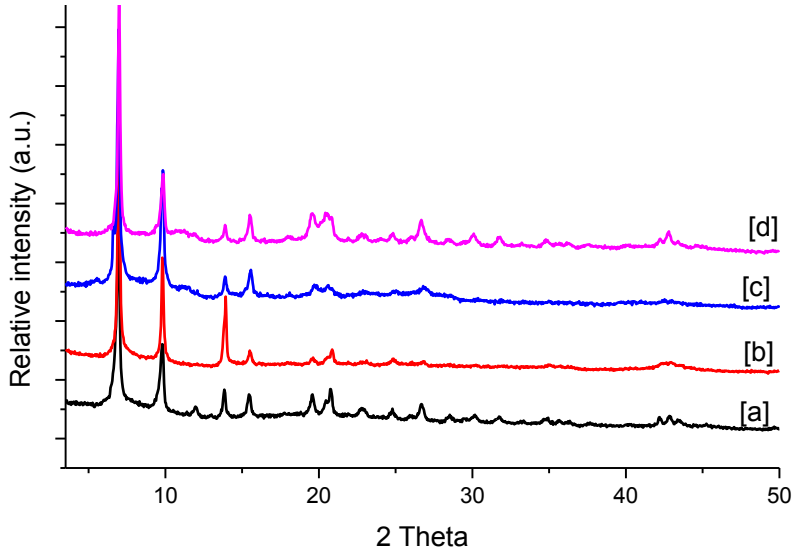

Fig. S1. Powder X-ray diffraction patterns of (a) IRMOF-3, (b) IRMOF-3-GL, (c) Nd-IRMOF-3-GL and (d) Eu-IRMOF-3-GL.

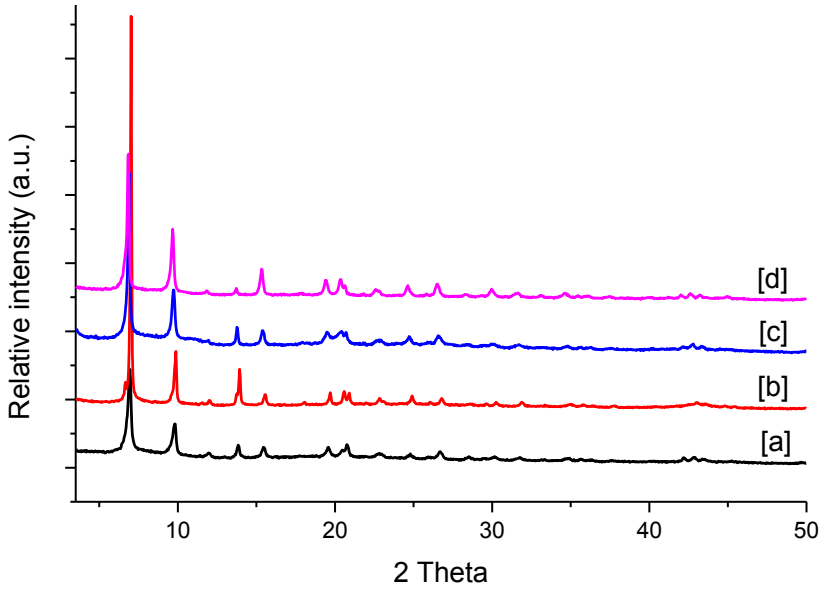

Fig. S2. Powder X-ray diffraction patterns of (a) IRMOF-3; (b) IRMOF-3-CA; (c) Nd-IRMOF-3-CA and (d) Eu-IRMOF-3-CA.

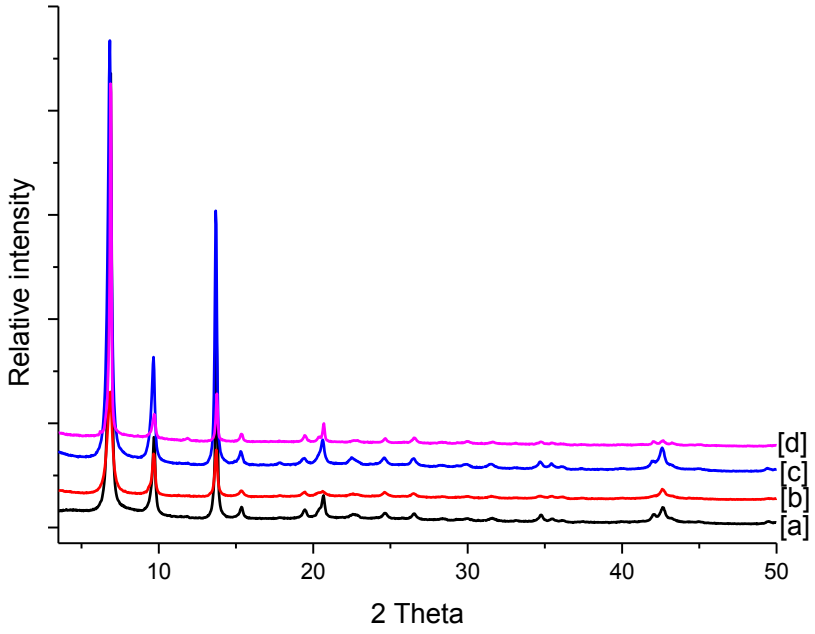

Fig. S3. Powder X-ray diffraction patterns of (a) IRMOF-3, (b) IRMOF-3-MVK, (c) Nd-IRMOF-3-MVK, (d) Eu-IRMOF-3-MVK.

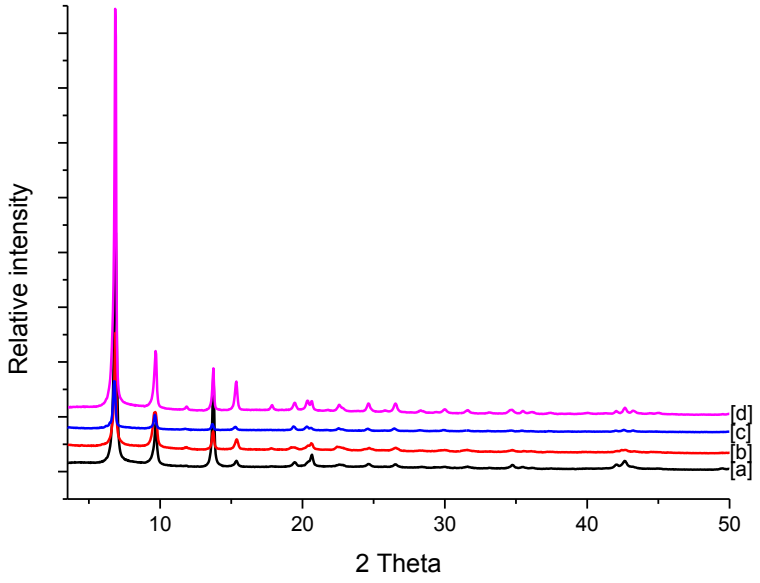

Fig. S4. Powder X-ray diffraction patterns of (a) IRMOF-3, (b) IRMOF-3-EM, (c) Nd-IRMOF-3-EM, (d) Eu-IRMOF-3-EM.

3. NMR analysis

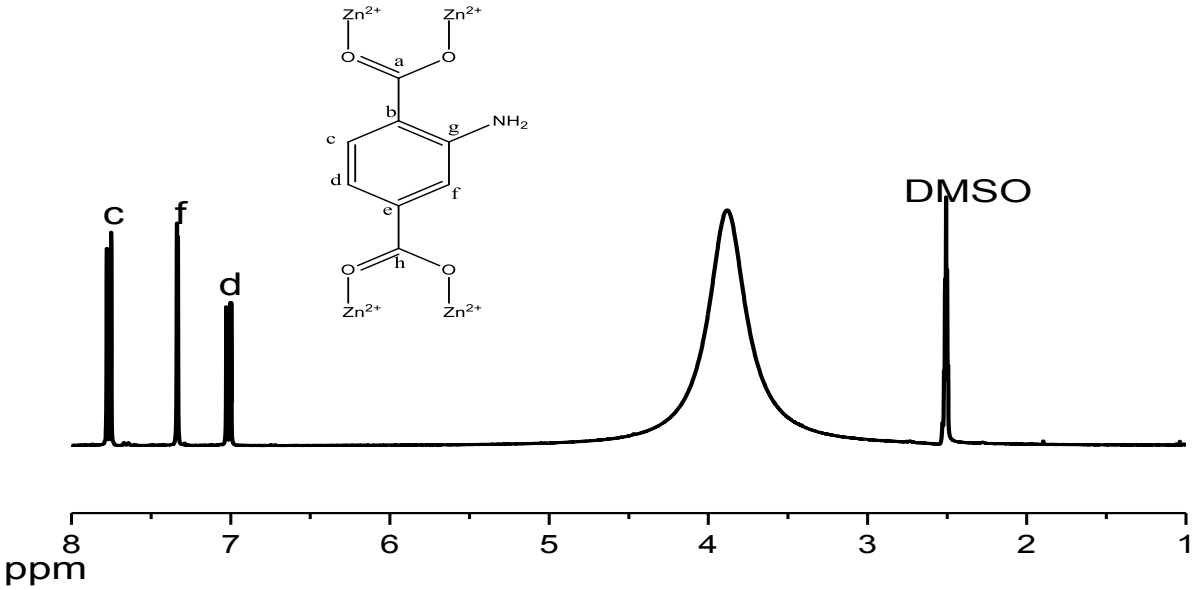

Fig. S5. ^{1}H NMR spectrum of IRMOF-3.

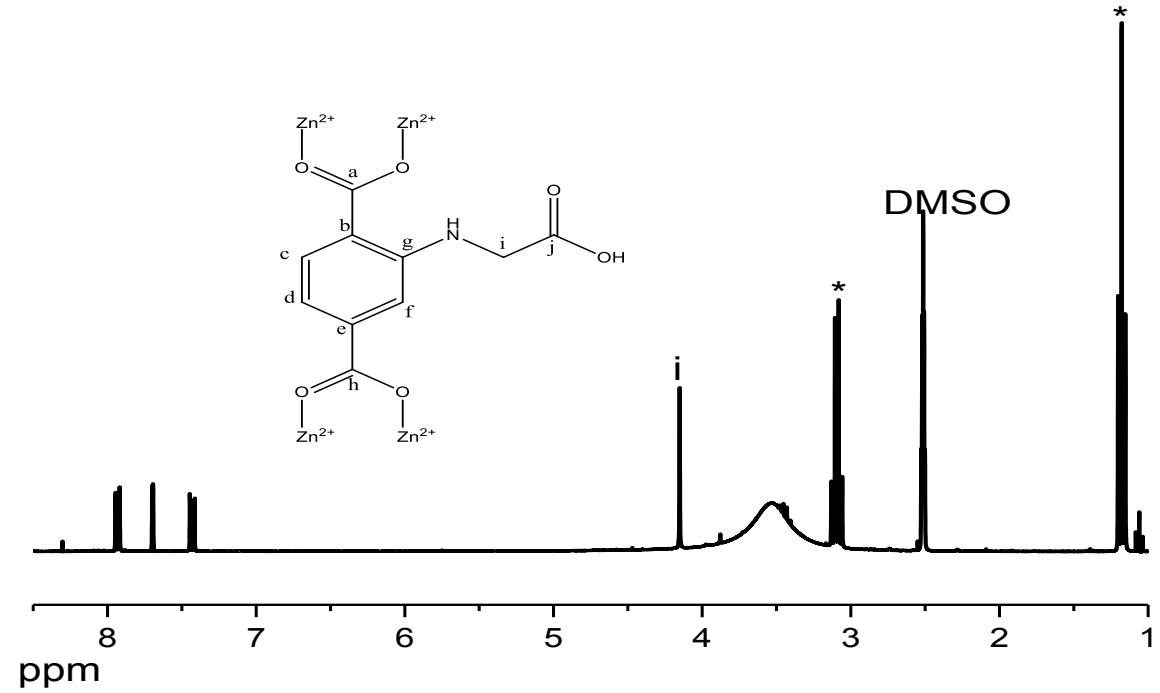

Fig. S6. ^{1}H NMR spectrum of IRMOF-3-CA, *= triethylamine

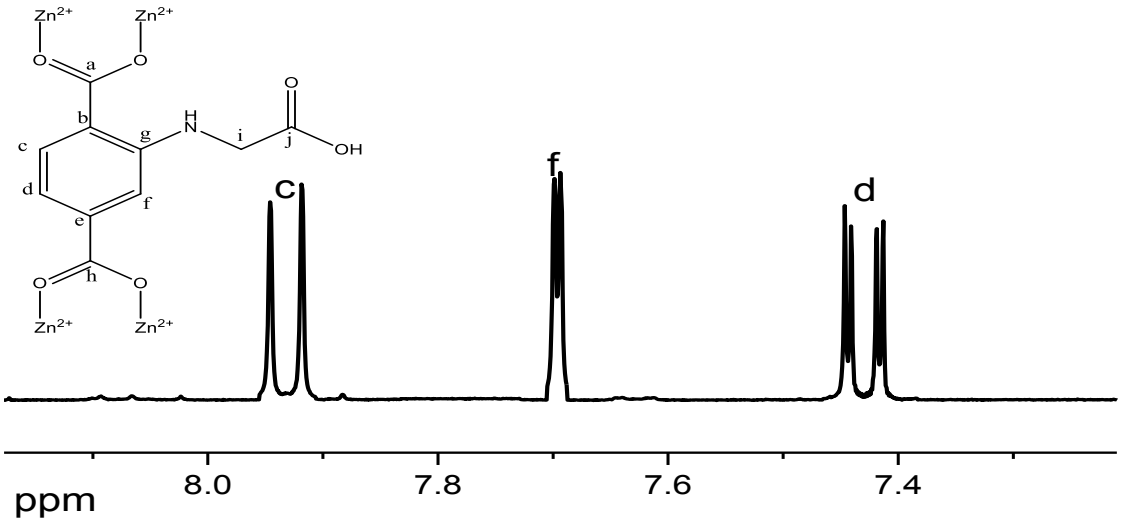

Fig. S7. Aromatic region of the ^{1}H NMR of spectrum IRMOF-3-CA.

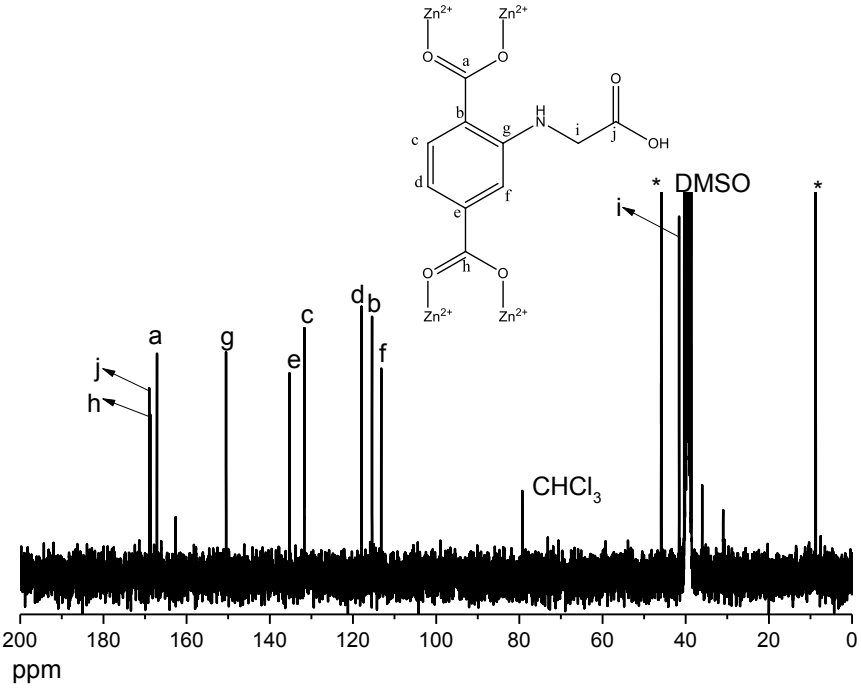

Fig. S8. ^{13}C NMR spectrum of IRMOF-3-CA, *triethylamine.

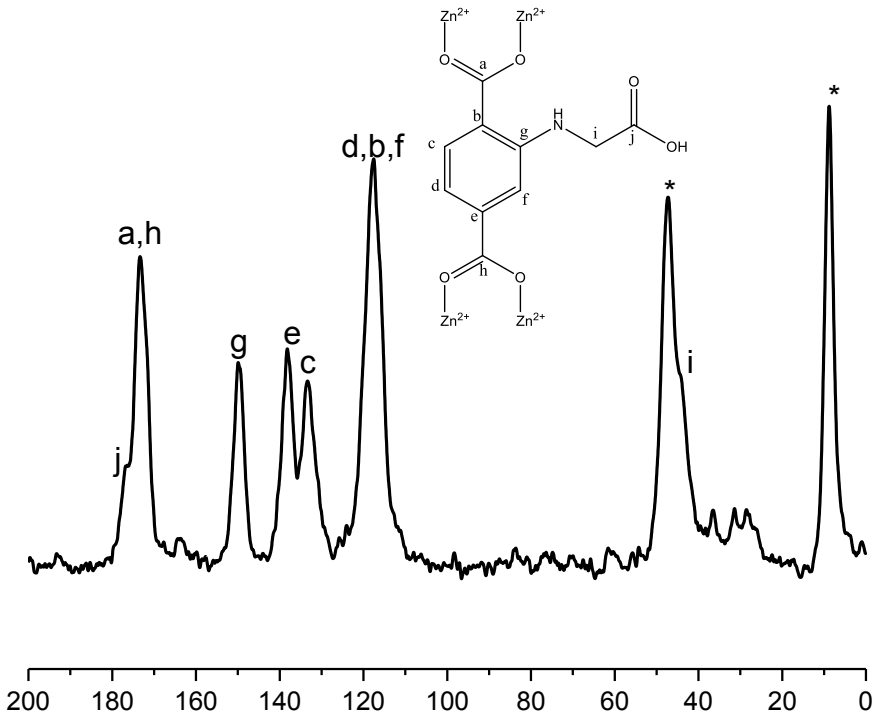

Fig. S9. Solid-state ^{13}C CP/MAS NMR spectrum of IRMOF-3-CA, *triethylamine.

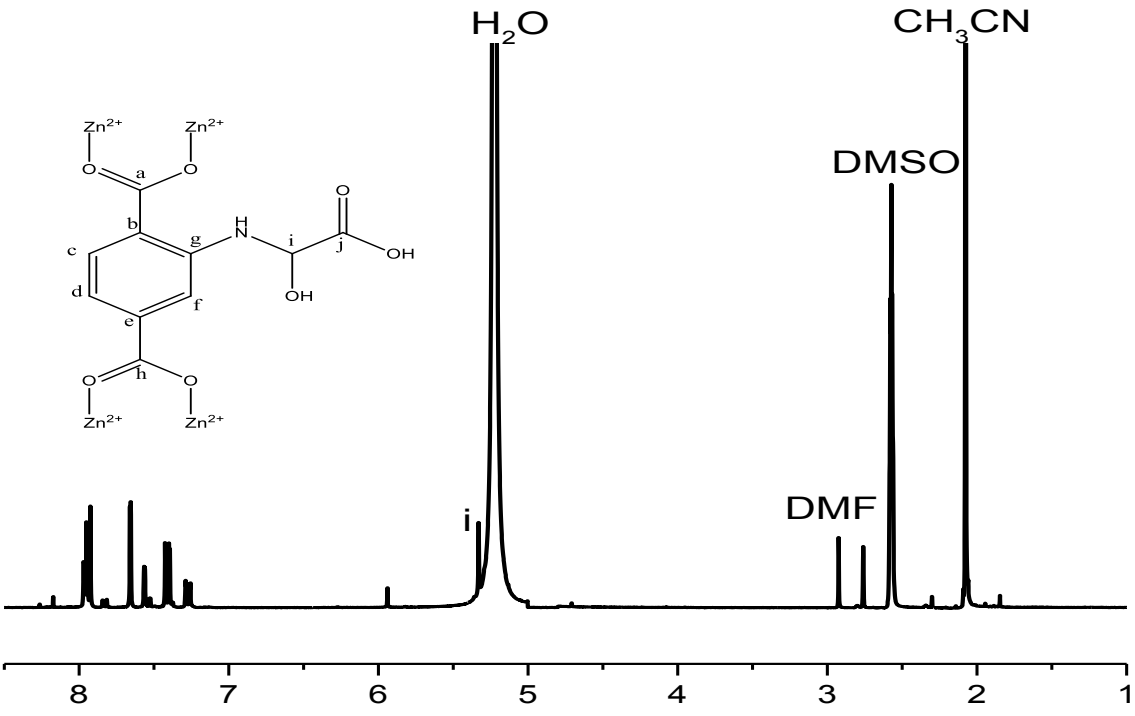

Fig. S10. ^{1}H NMR spectrum of IRMOF-3-Gl.

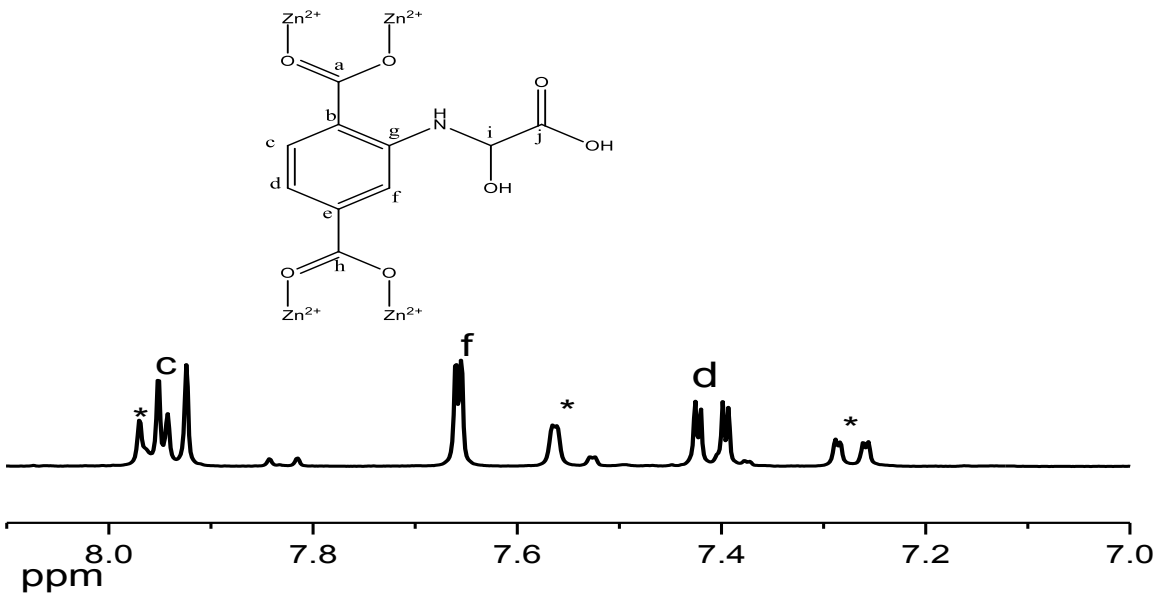

Fig. S11. Aromatic region of the ^{1}H NMR spectrum of IRMOF-3-Gl. * Unmodified IRMOF-3.

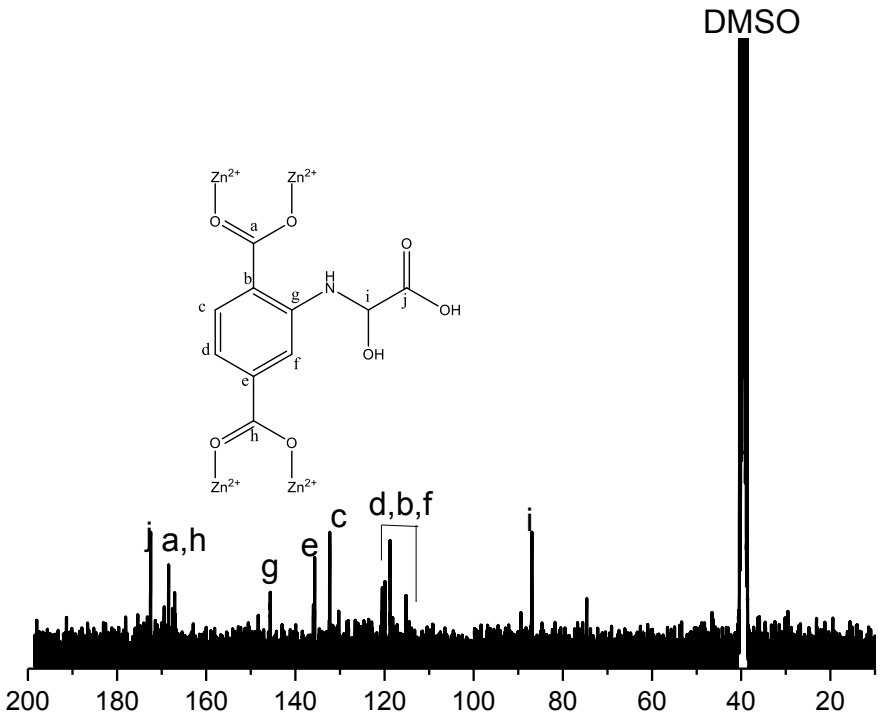

Fig. S12. ^{13}C NMR spectrum of IRMOF-3-GL.

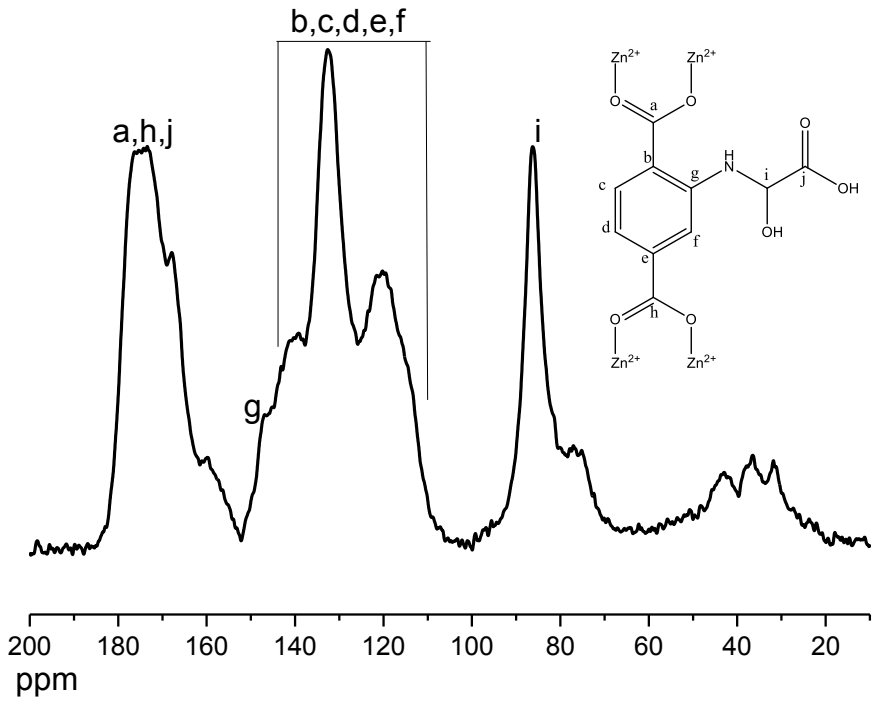

Fig. S13. Solid-state ^{13}C CP/MAS NMR spectrum of IRMOF-3-Gl.

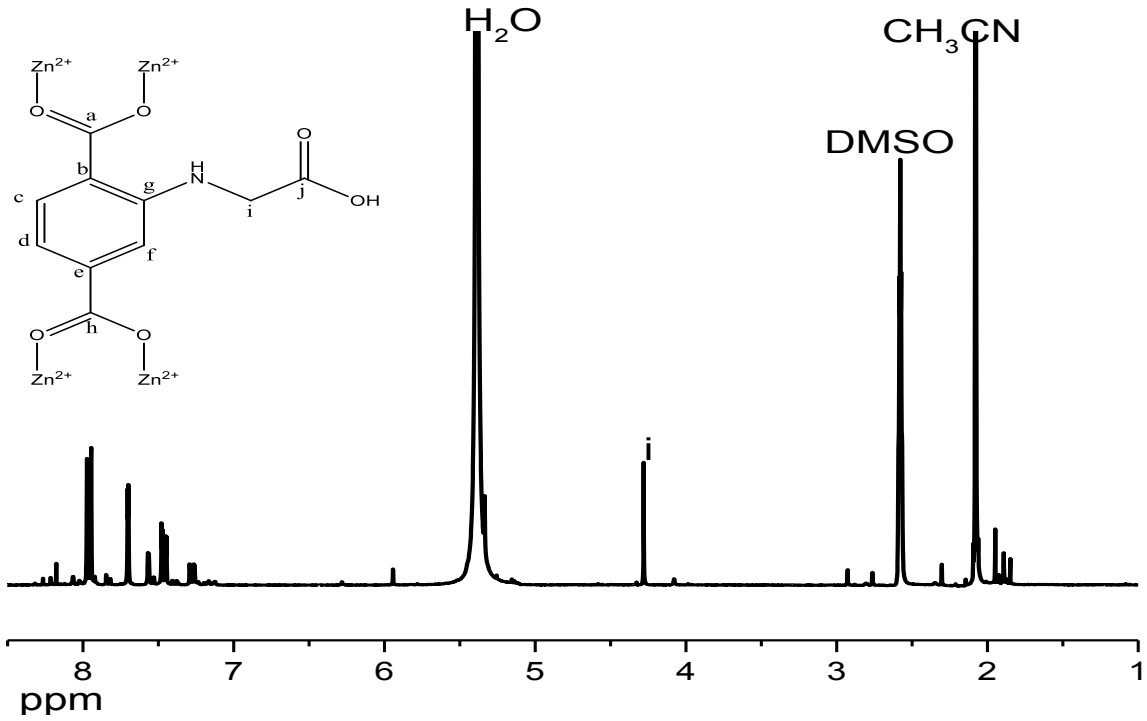

Fig. S14. ^{1}H NMR spectrum of IRMOF-3-Gl-R.

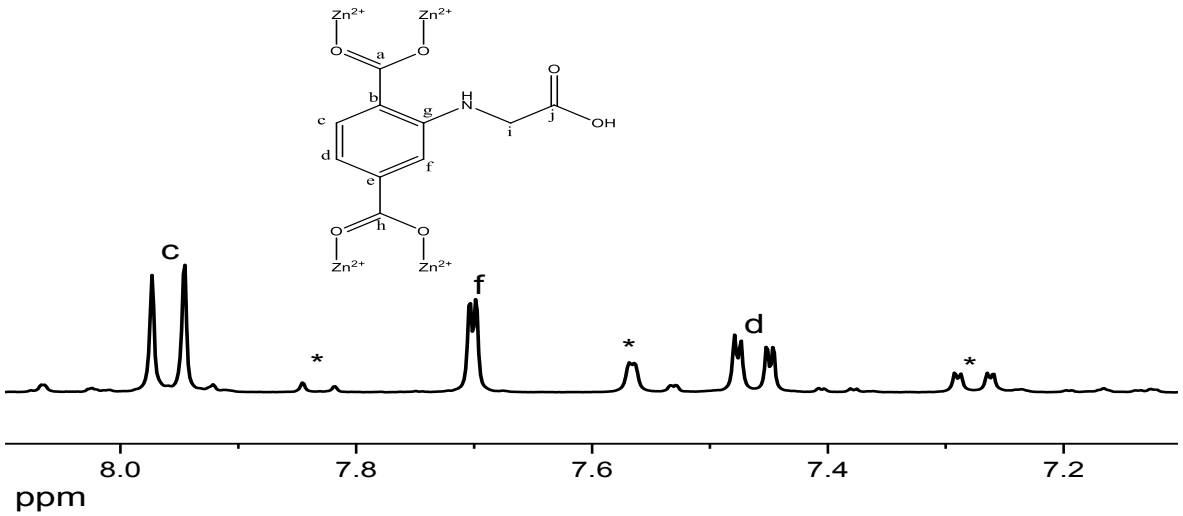

Fig. S15. Aromatic region of the ^{1}H NMR spectrum of IRMOF-3-Gl-R. * Unmodified IRMOF-3.

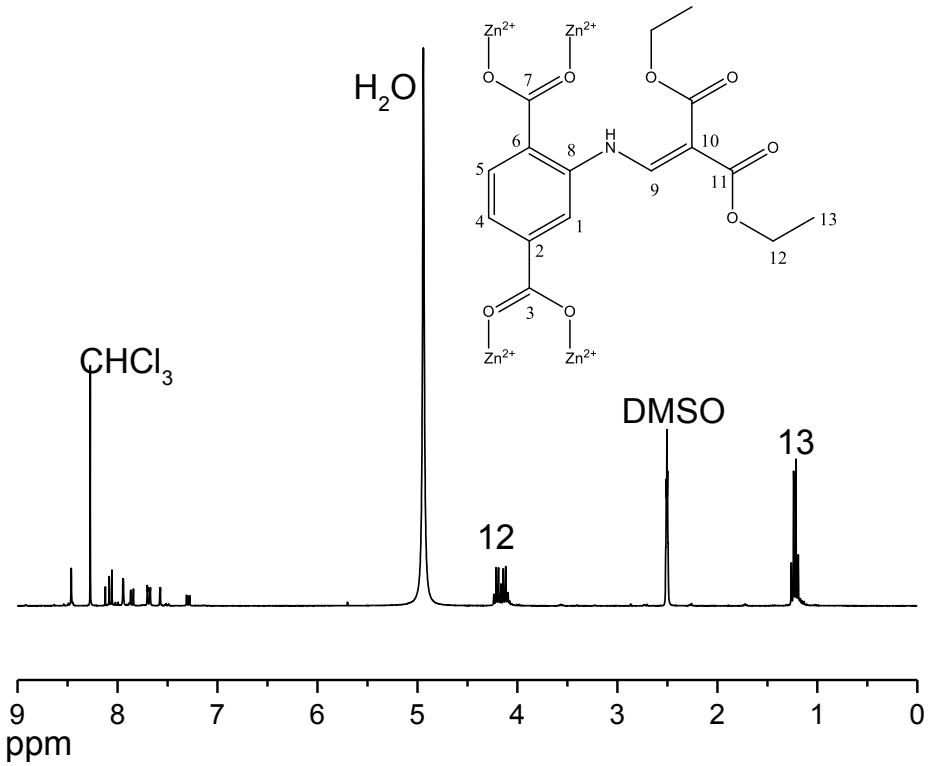

Fig. S16. ^{1}H NMR spectrum of IRMOF-3-EM.

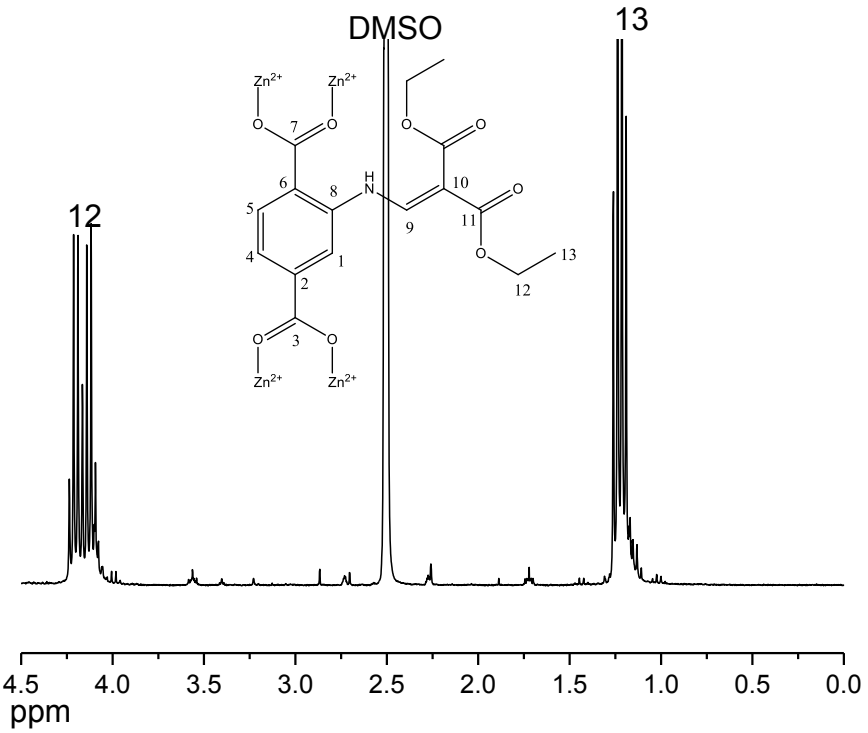

Fig. S17. Aliphatic region of the ^{1}H NMR spectrum of IRMOF-3-EM.

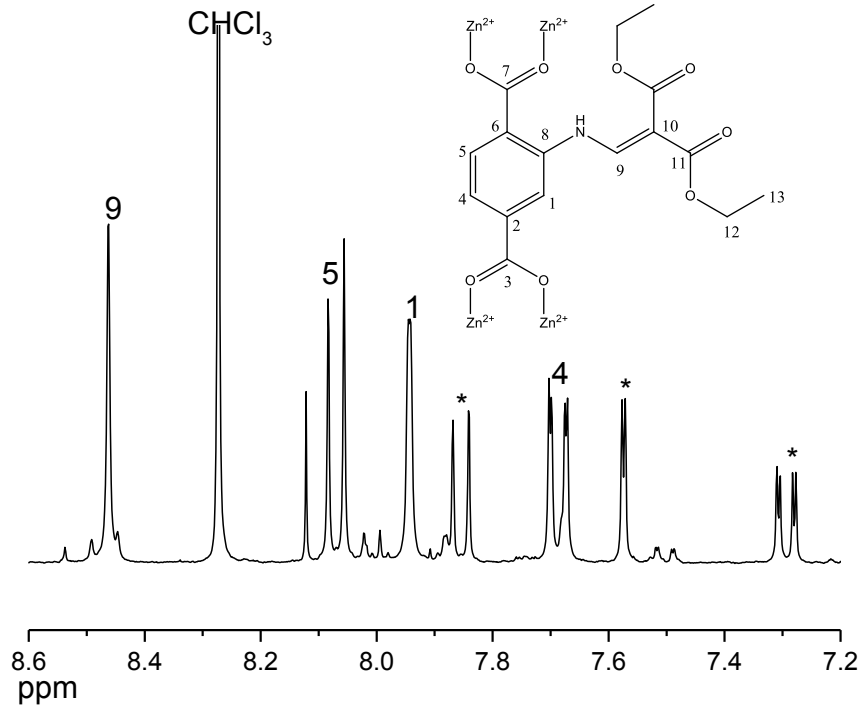

Fig. S18. Aromatic region of the ^{1}H NMR spectrum of IRMOF-3-EM. * Unmodified IRMOF-3.

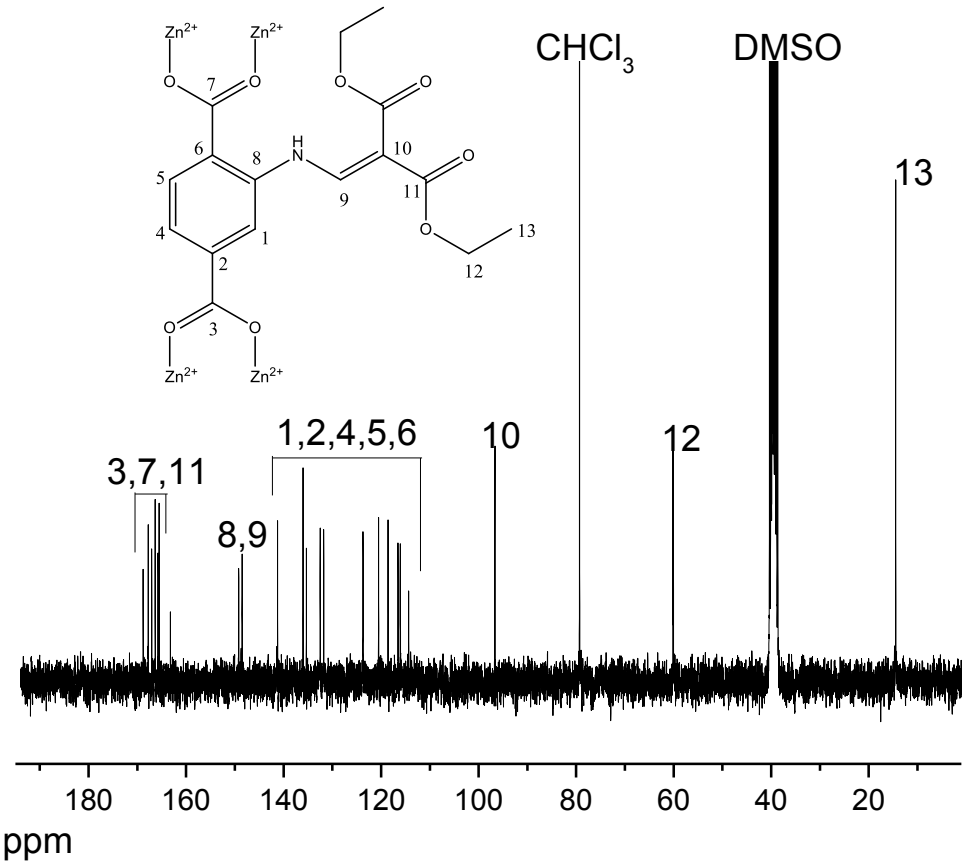

Fig. S19. ^{13}C NMR spectrum of IRMOF-3-EM.

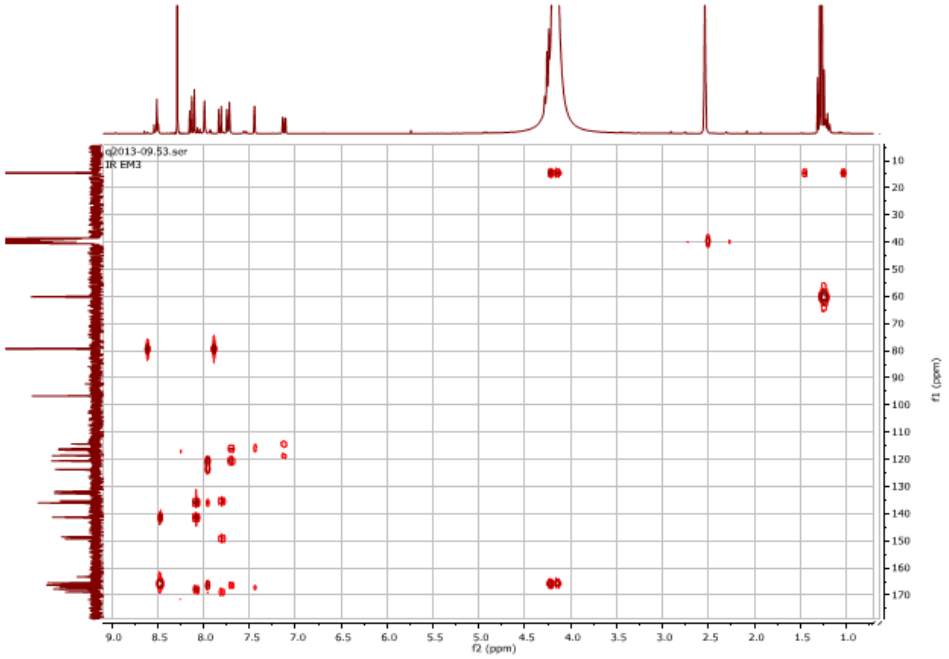

Fig. S20. HMBC spectrum of IRMOF-3-EM.

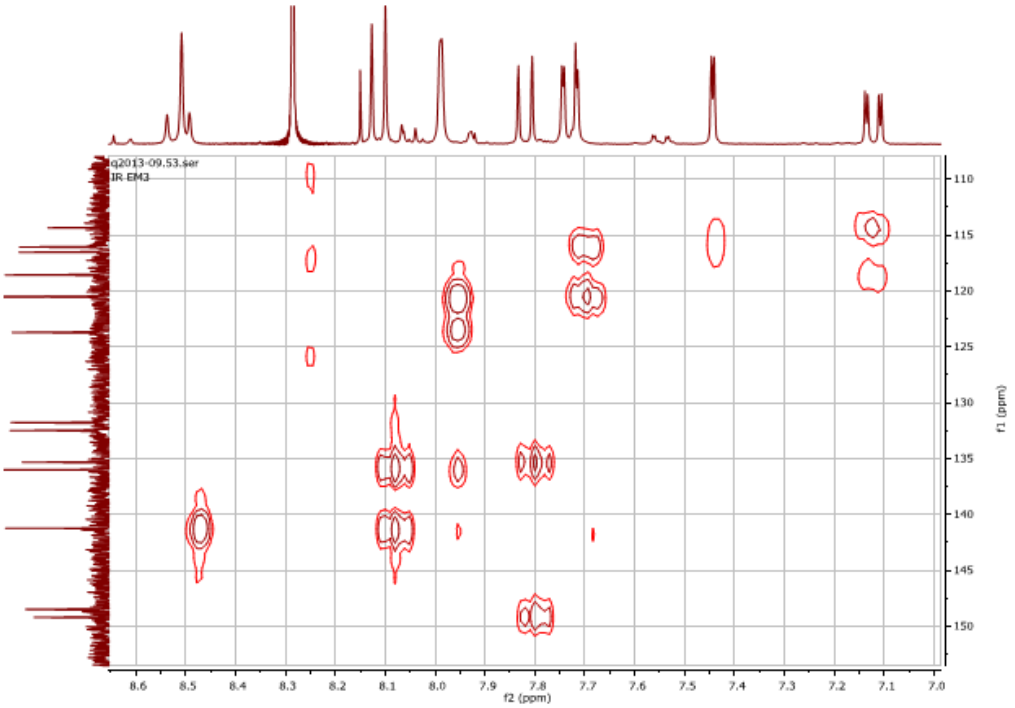

Fig. S21. Expansion of HMBC spectrum of IRMOF-3-EM.

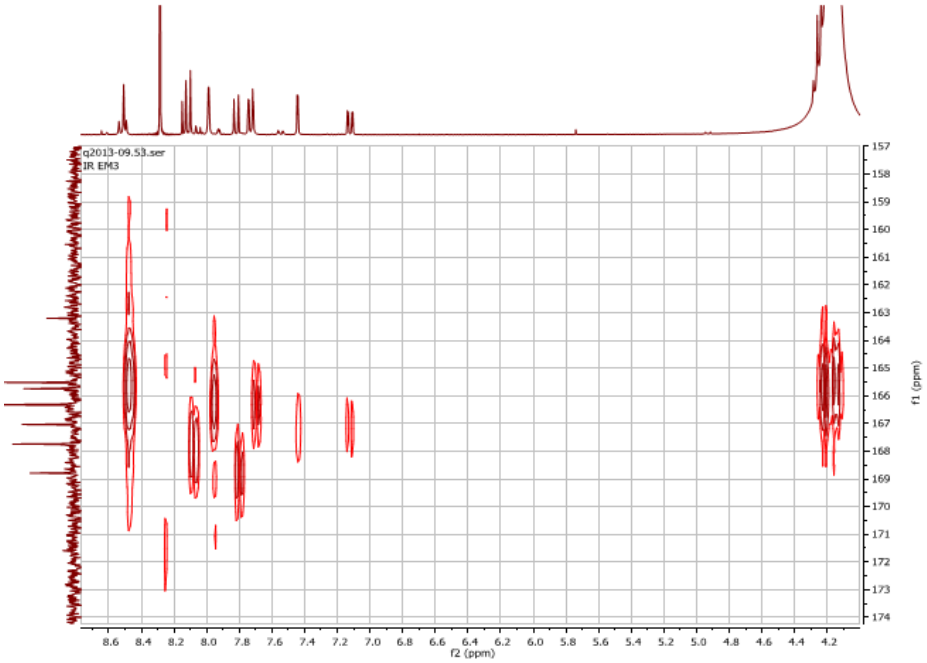

Fig. S22. Expansion of HMBC spectrum of IRMOF-3-EM.

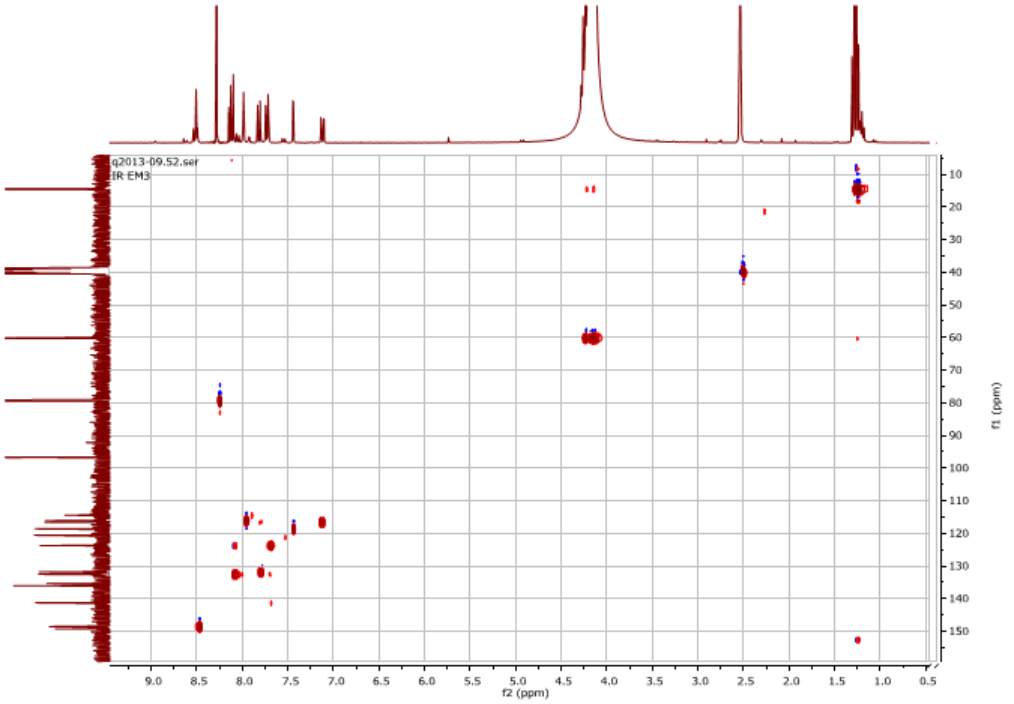

Fig. S23. Expansion of HSQC spectrum of IRMOF-3-EM.

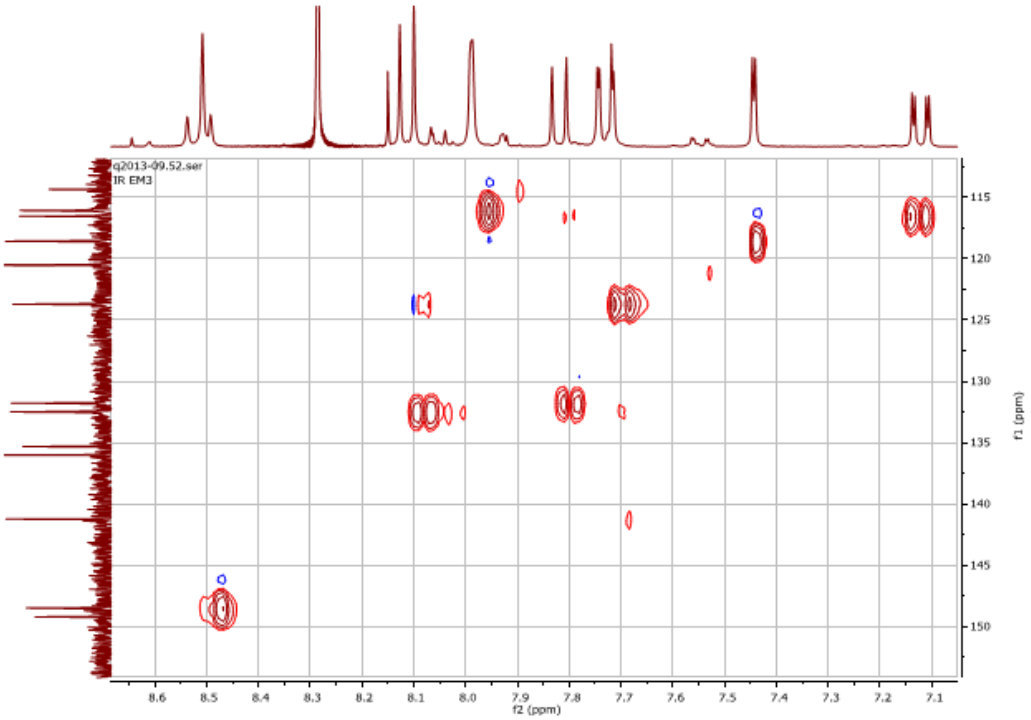

Fig. S24. Expansion of HSQC spectrum of IRMOF-3-EM.

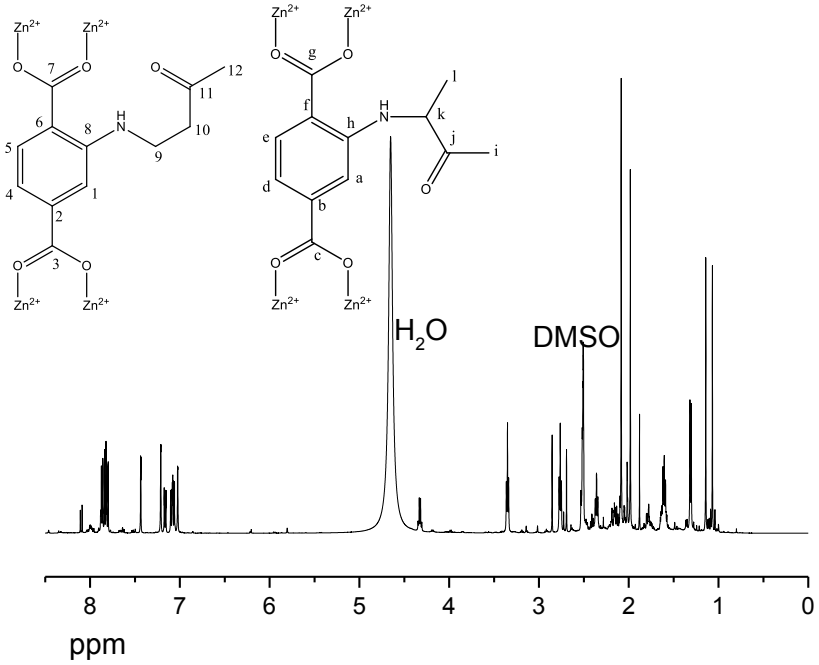

Fig. S25. ^{1}H NMR spectrum of IRMOF-3-MVK.

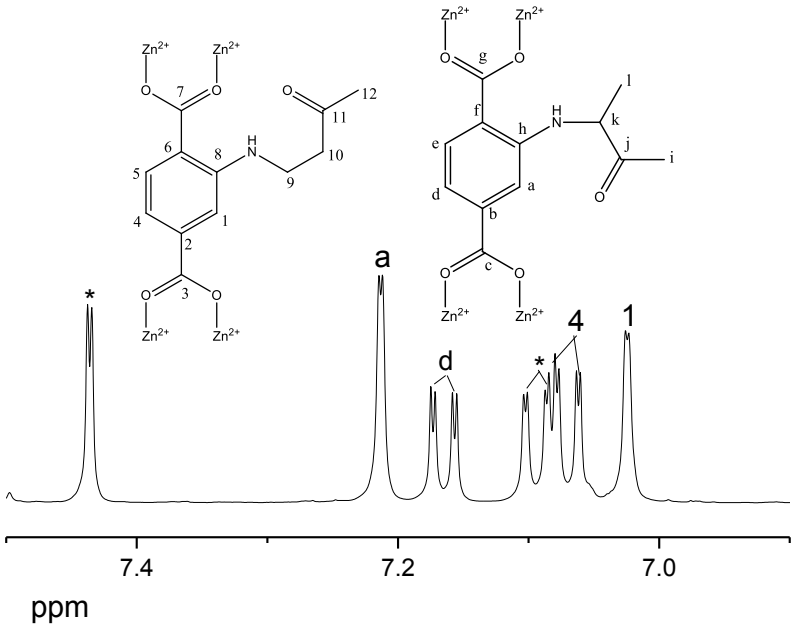

Fig. S26. Expansion of the aromatic region of the ^{1}H NMR spectrum of IRMOF-3-MVK. * Unmodified IRMOF-3.

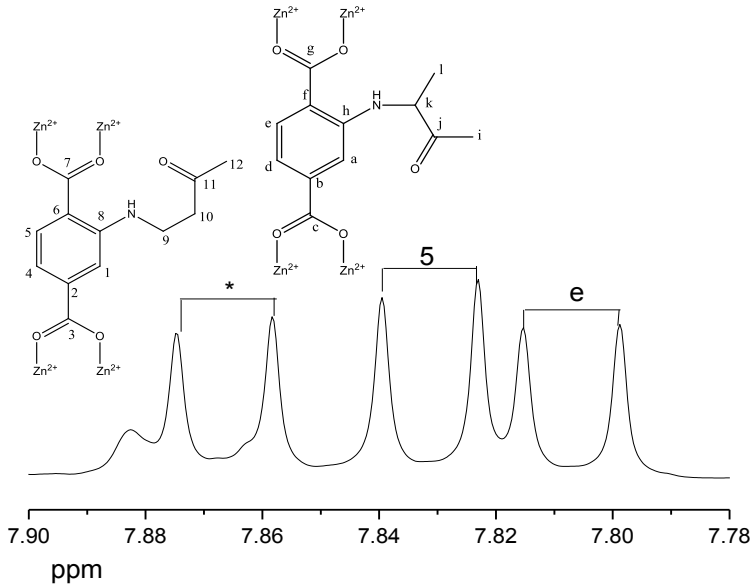

Fig. S27. Expansion of the aromatic region of the ^{1}H NMR spectrum of IRMOF-3-MVK. * Unmodified IRMOF-3.

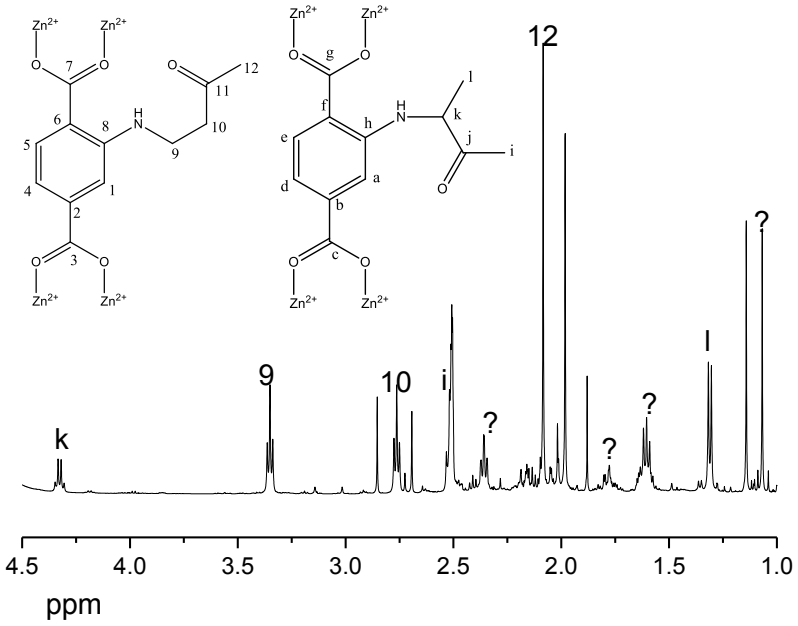

Fig. S28. Aliphatic region of the ^{1}H NMR spectrum of IRMOF-3-MVK. **?** = oligomers of MVK.

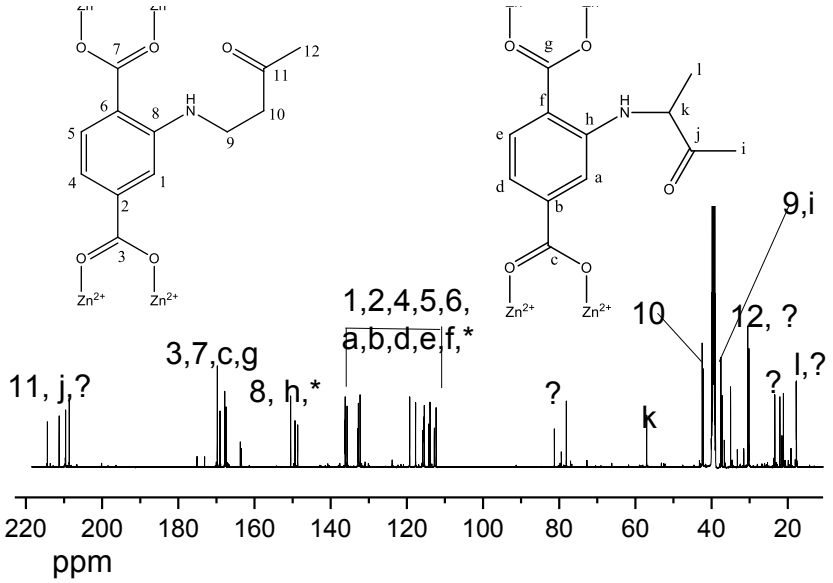

Fig. S29. ^{13}C NMR spectrum of IRMOF-3-MVK. **?** = oligomers of MVK. * Unmodified IRMOF-3.

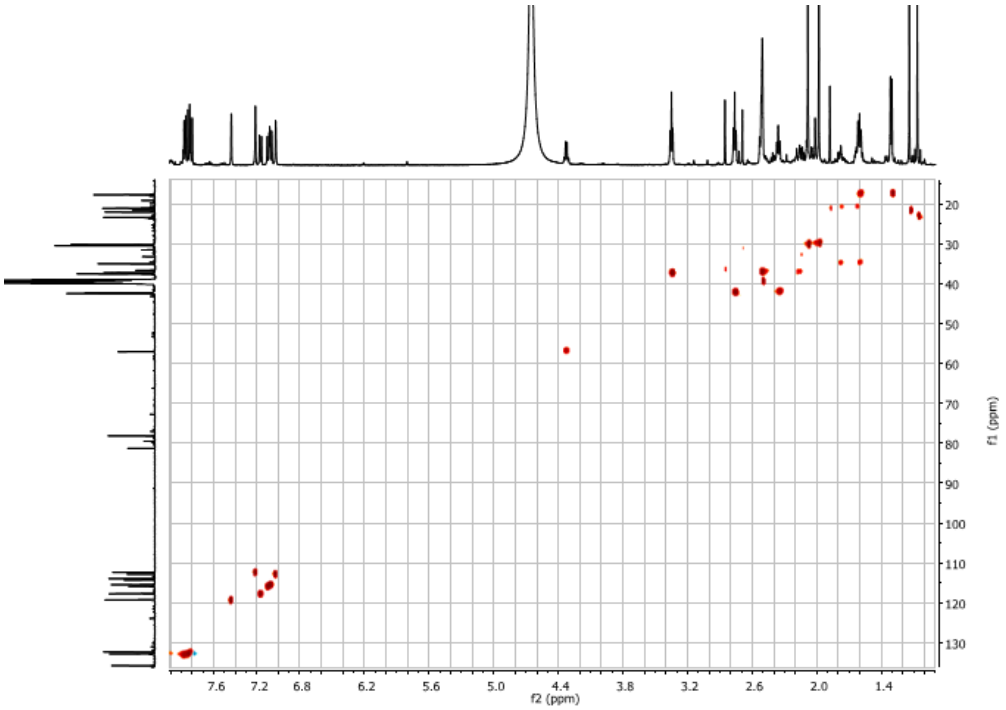

Fig. S30. HSQC spectrum of IRMOF-3-MVK

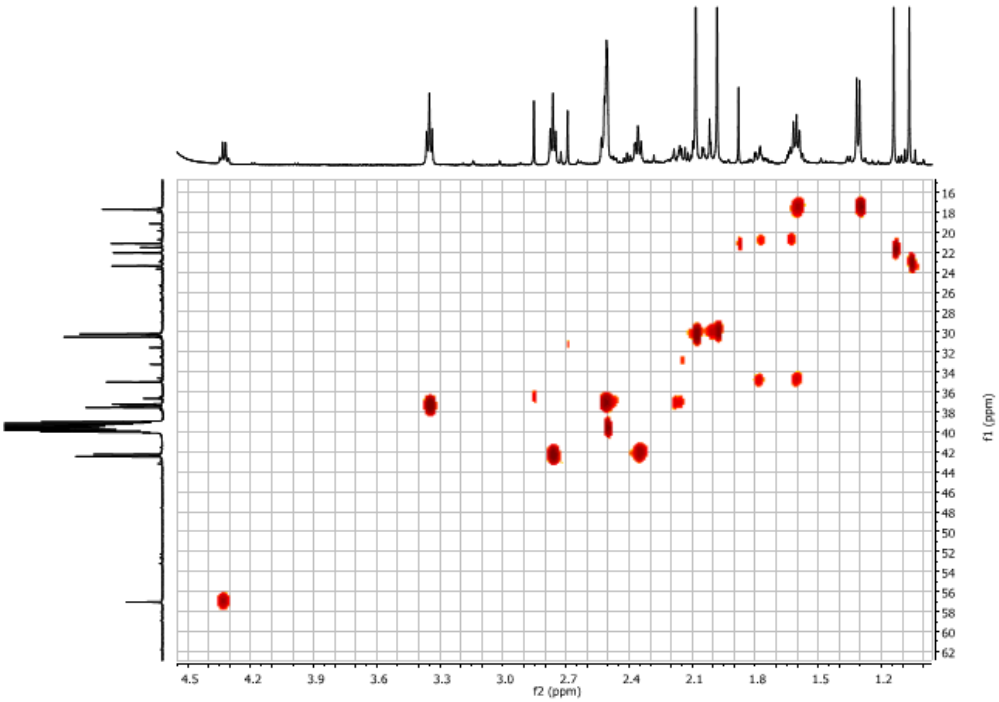

Fig. S31. Expansion of the HSQC spectrum of IRMOF-3-MVK.

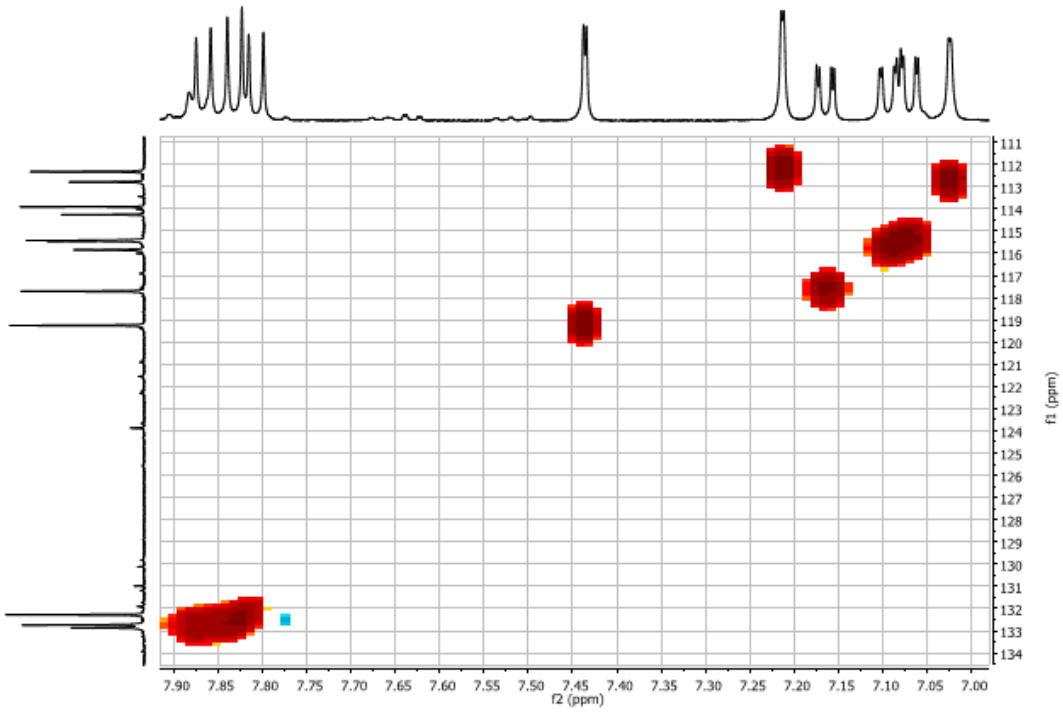

Fig. S32. Expansion of the HSQC spectrum of IRMOF-3-MVK.

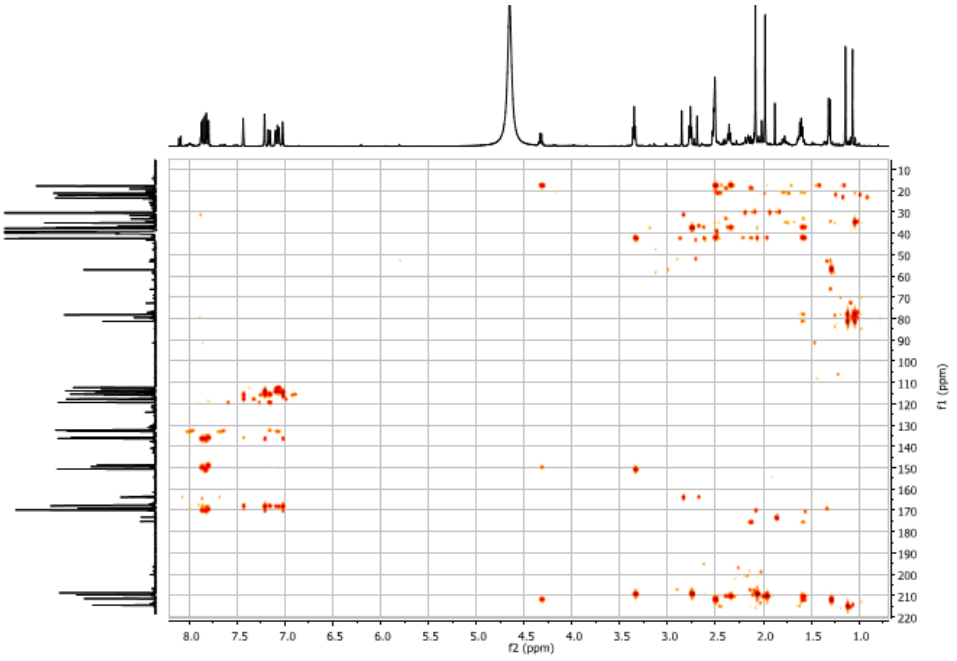

Fig. S33. HMBC spectrum of IRMOF-3-MVK.

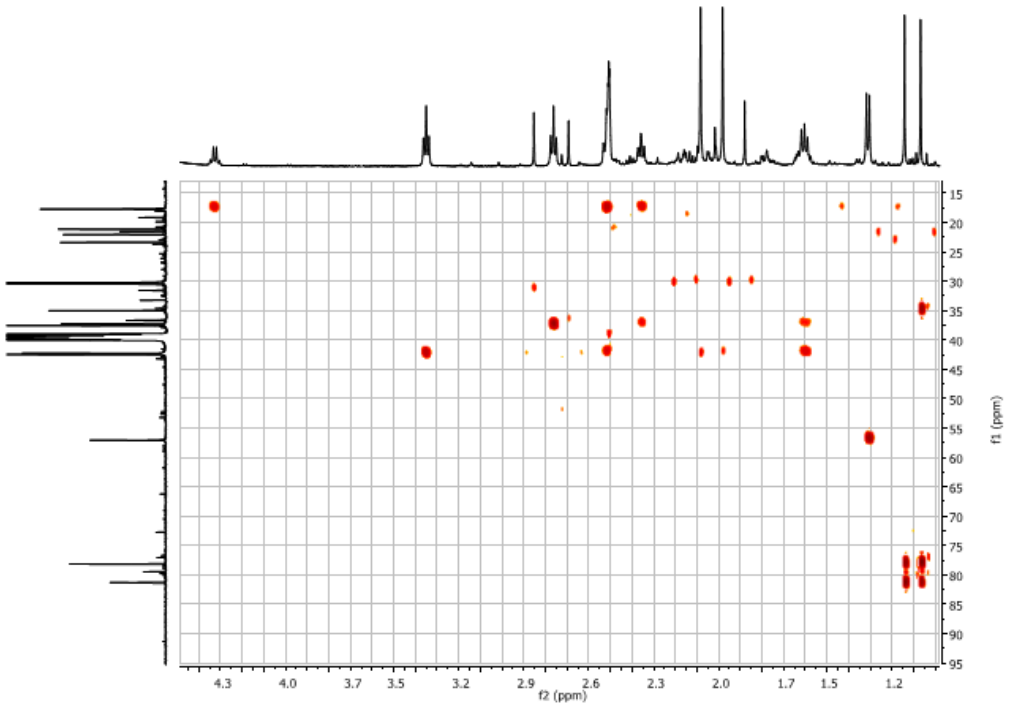

Fig. S34. Expansion of the HMBC spectrum of IRMOF-3-MVK.

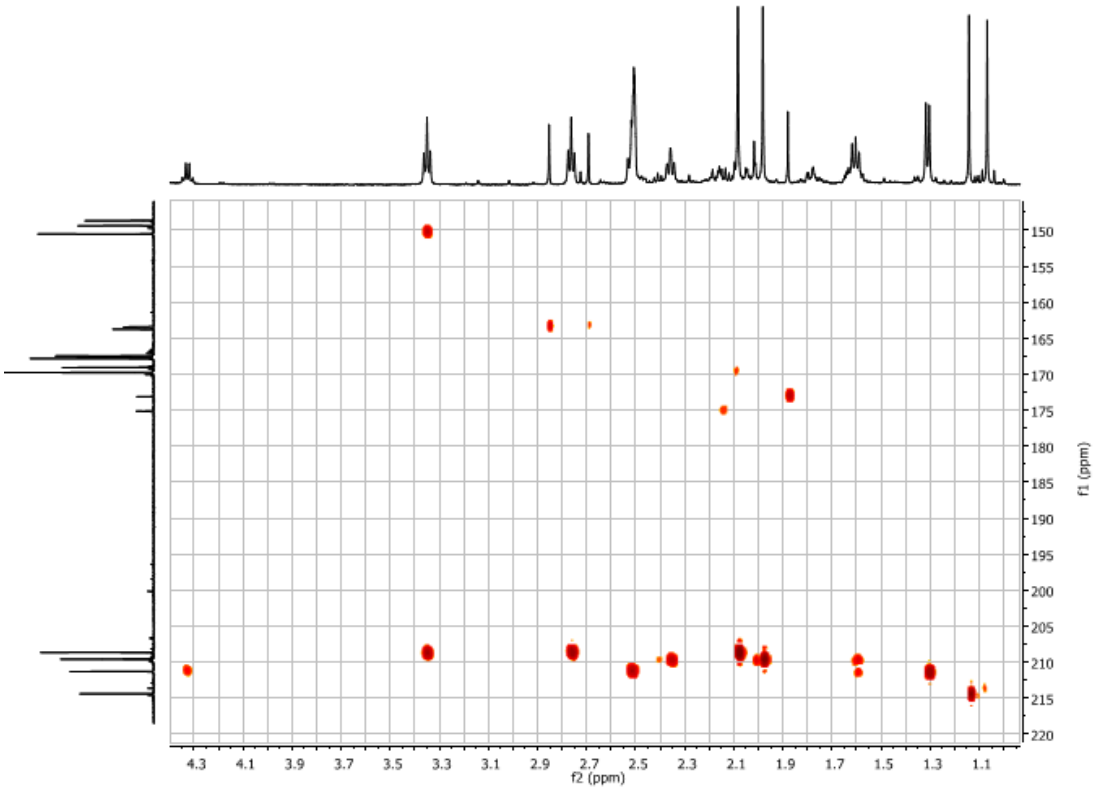

Fig. S35. Expansion of the HMBC spectrum of IRMOF-3-MVK.

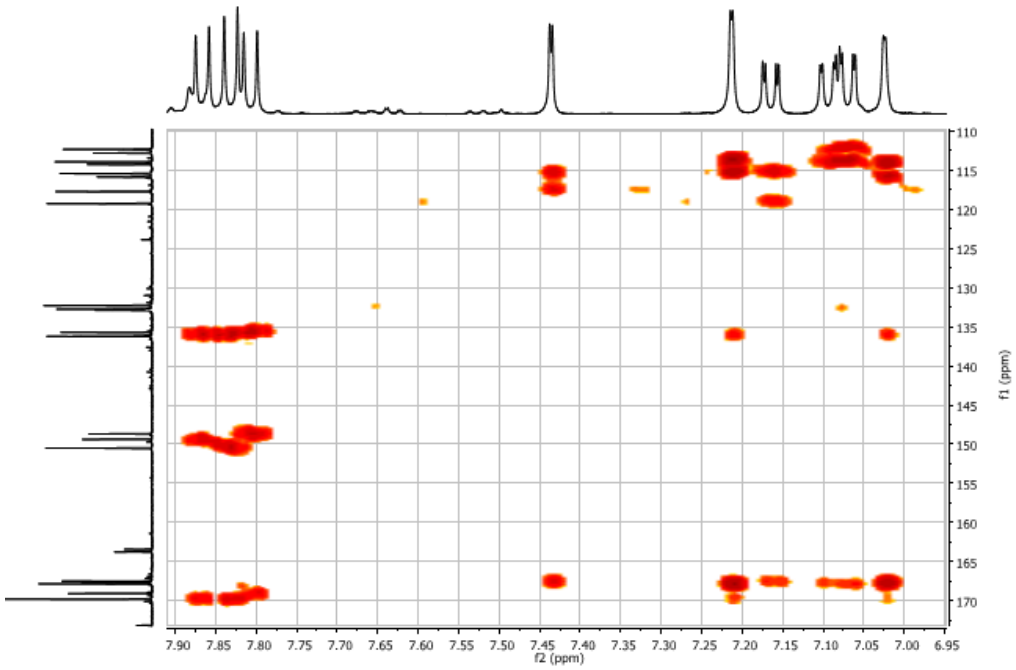

Fig. S36. Expansion of the HMBC spectrum of IRMOF-3-MVK.

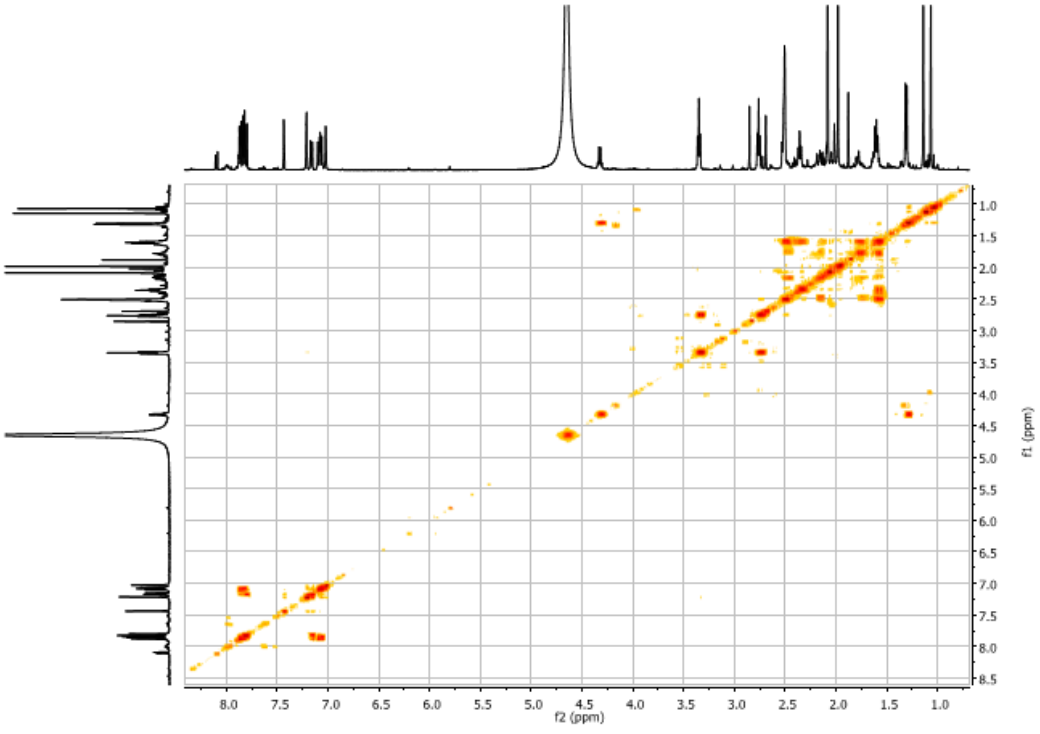

Fig. S37. 2D COSY spectrum of IRMOF-3-MVK.

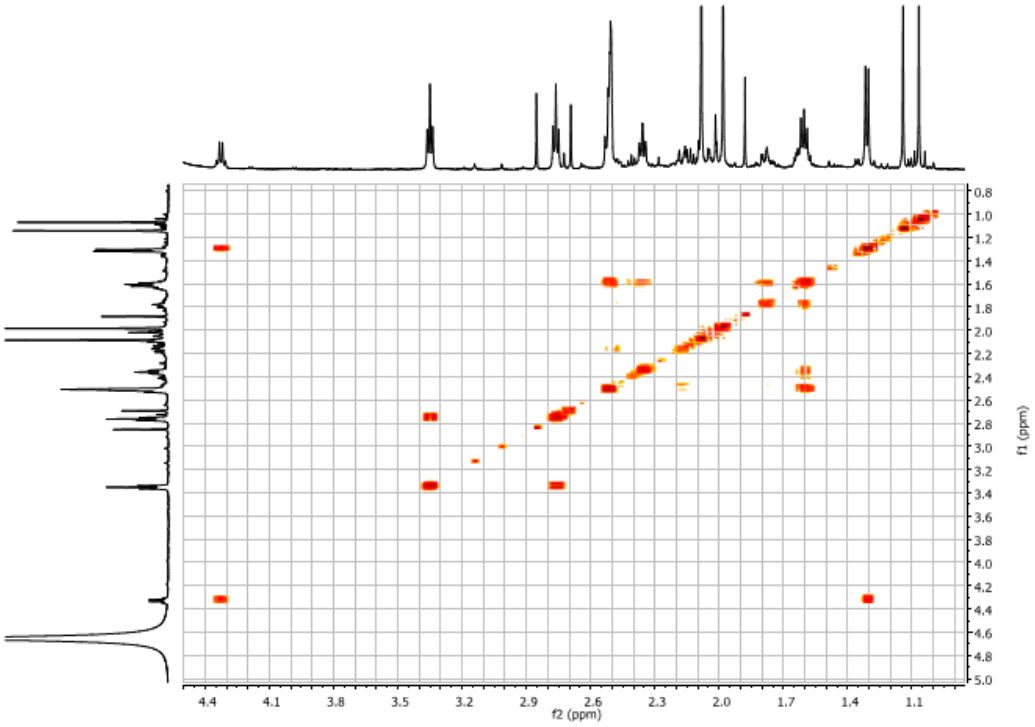

Fig. S38. Expansion of the 2D COSY spectrum of IRMOF-3-MVK.

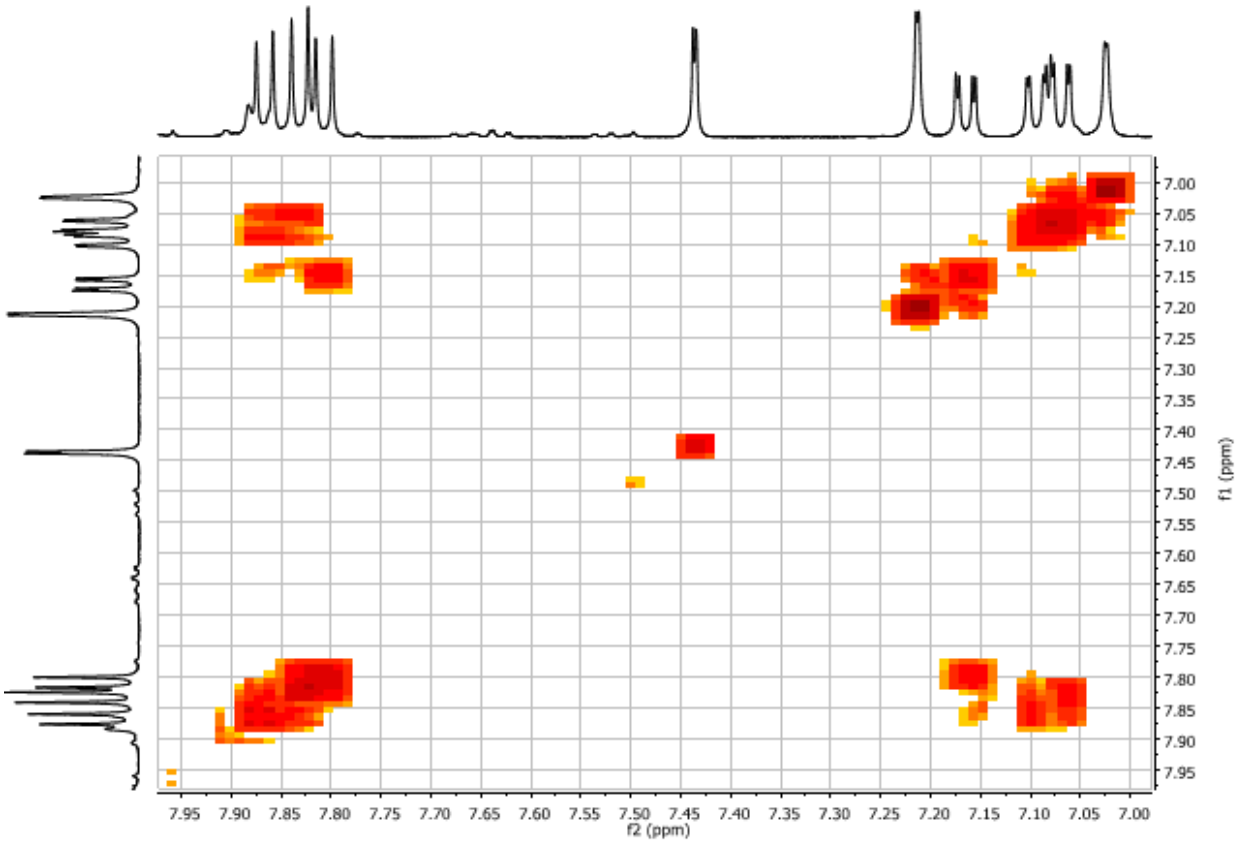

Fig. S39. Expansion of the 2D COSY spectrum of IRMOF-3-MVK.

4. FT-IR analysis

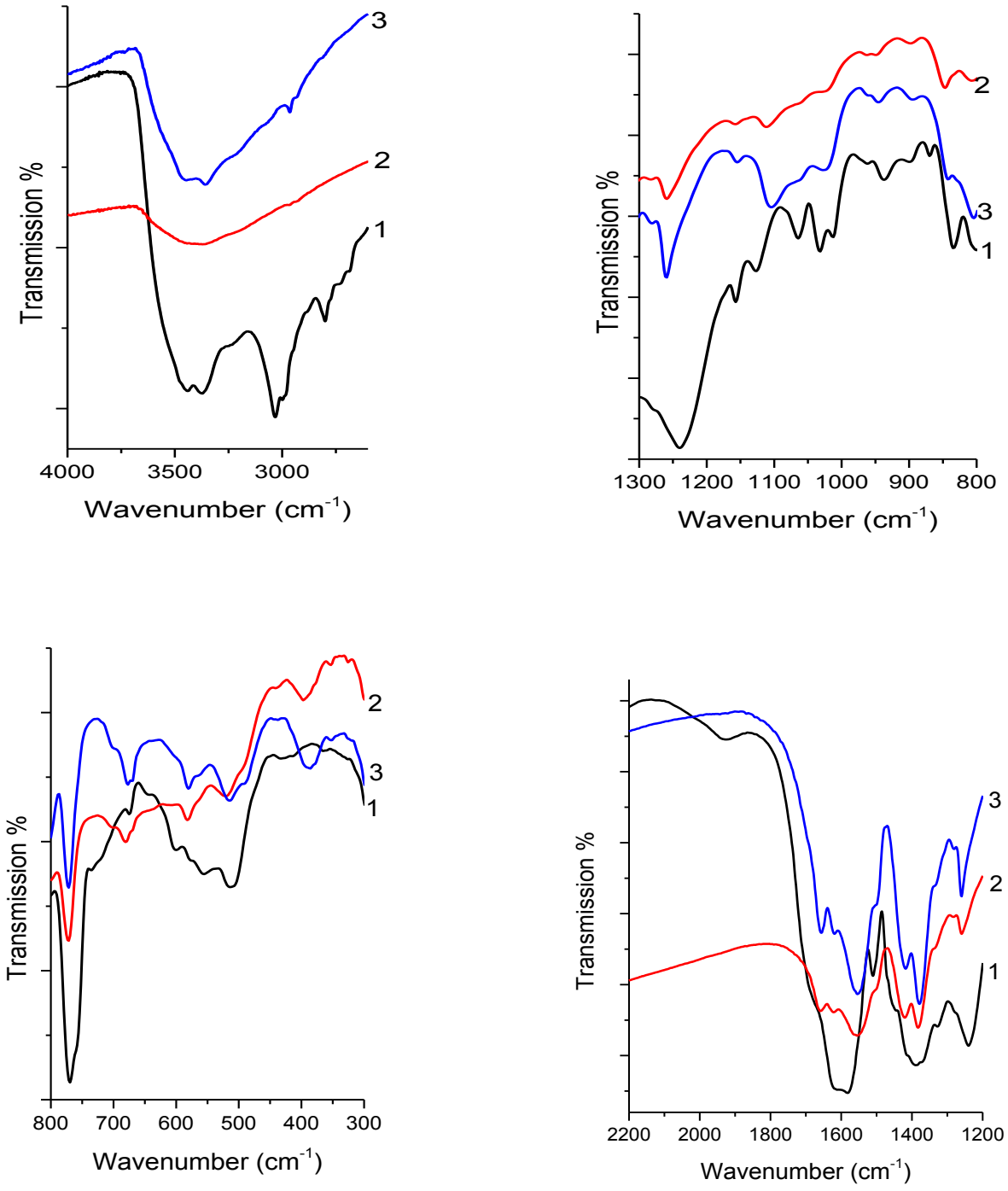

Fig. S40. FTIR spectra of (1) IRMOF-3-CA, (2) IRMOF-3-CA-Nd and (3) IRMOF-3-CA-Eu.

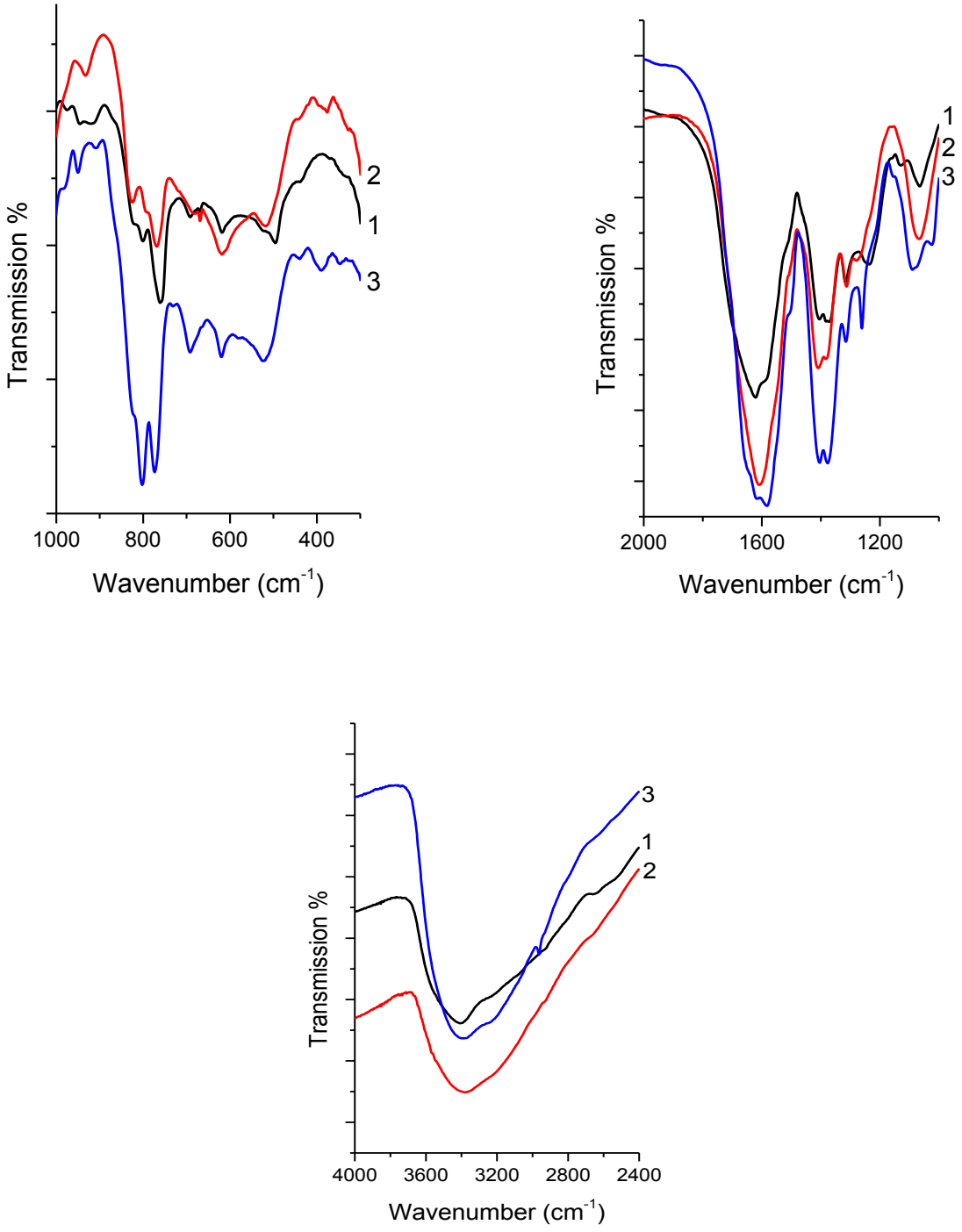

Fig. S41 FTIR spectra of (1) IRMOF-3-GL, (2) Nd-IRMOF-3-GL and (3) Eu-IRMOF-3-GL.

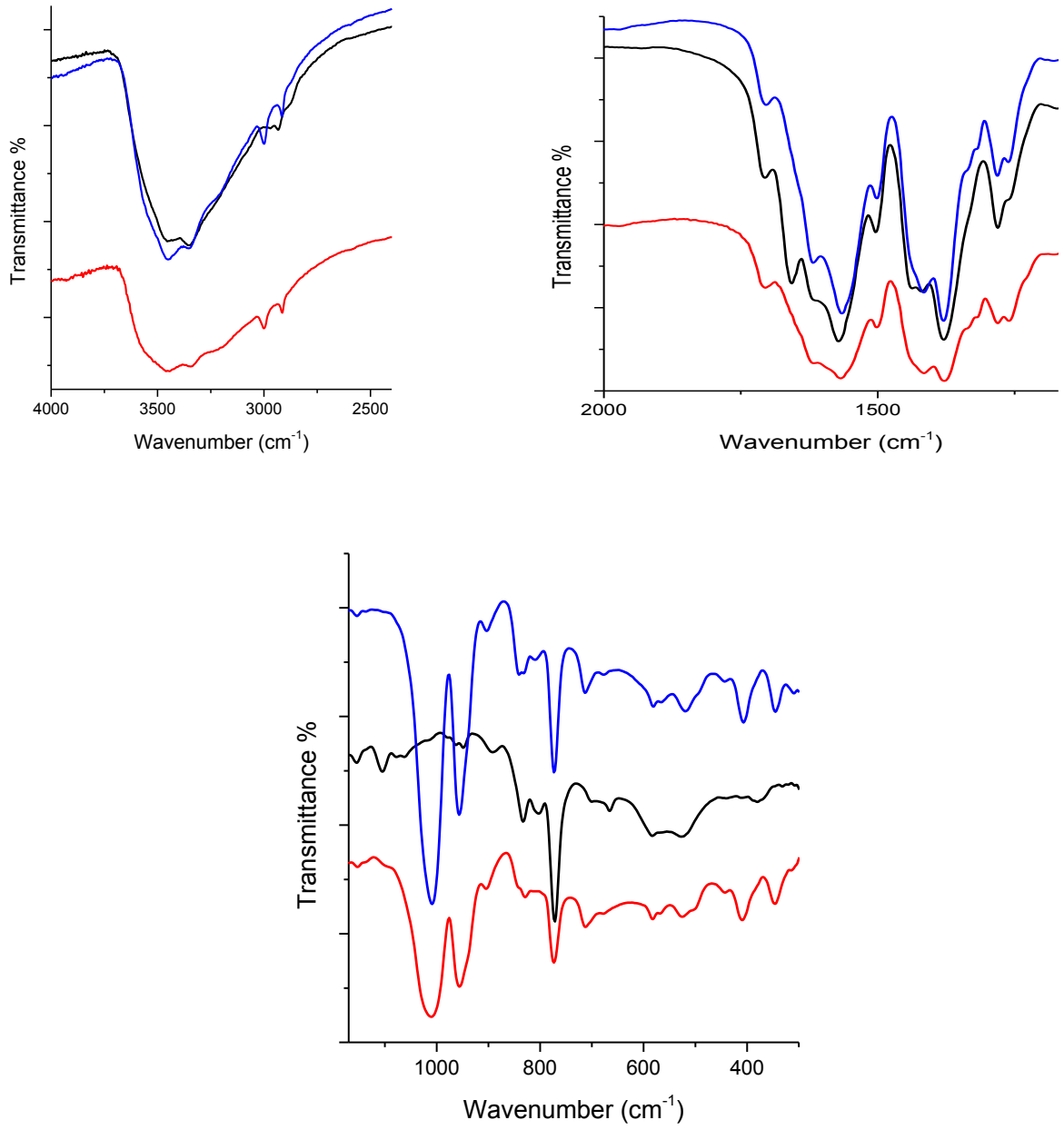

Fig. S42. FTIR spectra of IRMOF-3-MVK (black), Eu-IRMOF-3-MVK (red), and Nd-IRMOF-3-MVK (blue).

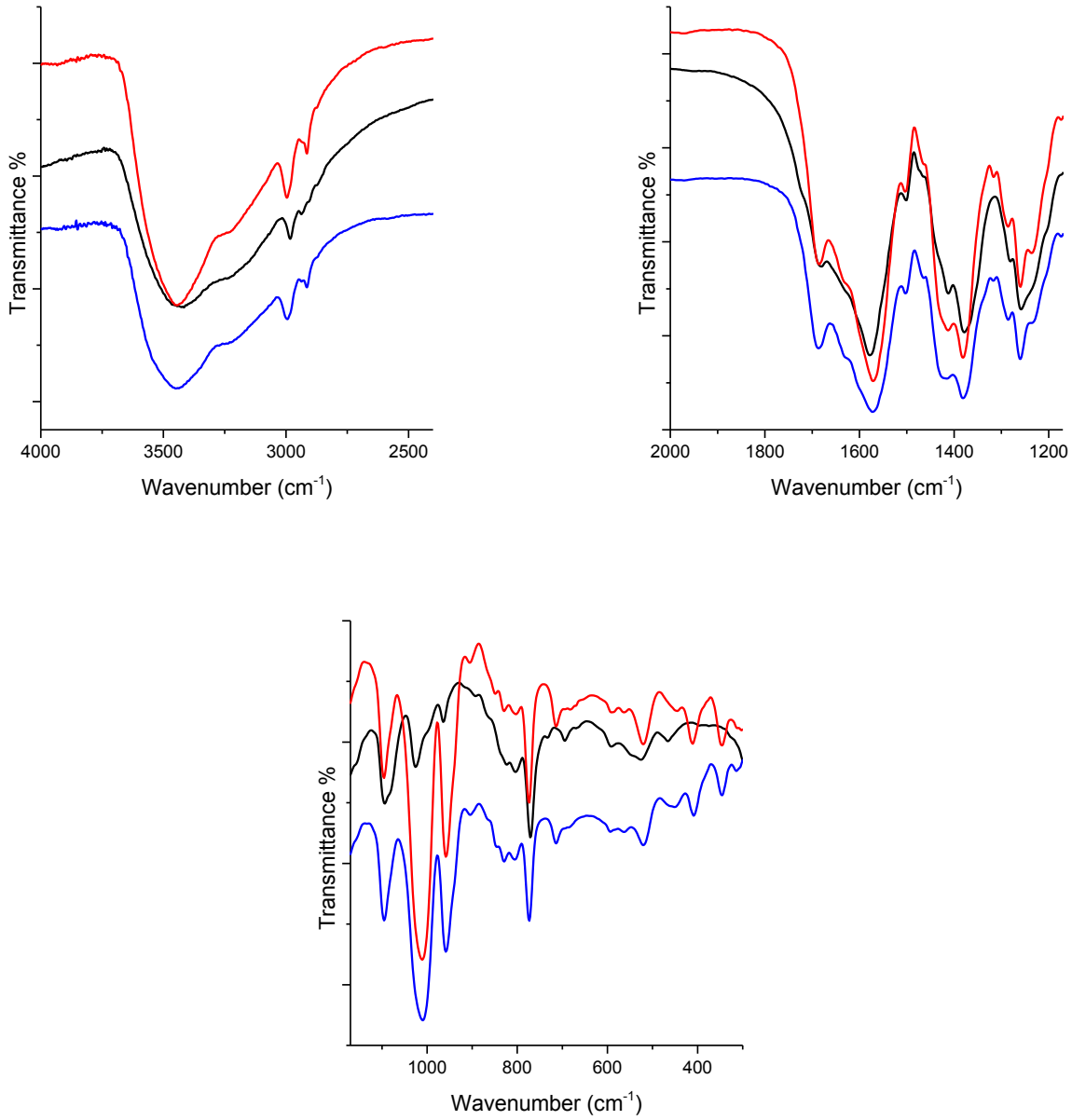

Fig. S43. FTIR spectra of IRMOF-3-EM (black), Eu-IRMOF-3-EM (red), and Nd-IRMOF-3-EM (blue).

5. Scanning Electron Microscopy

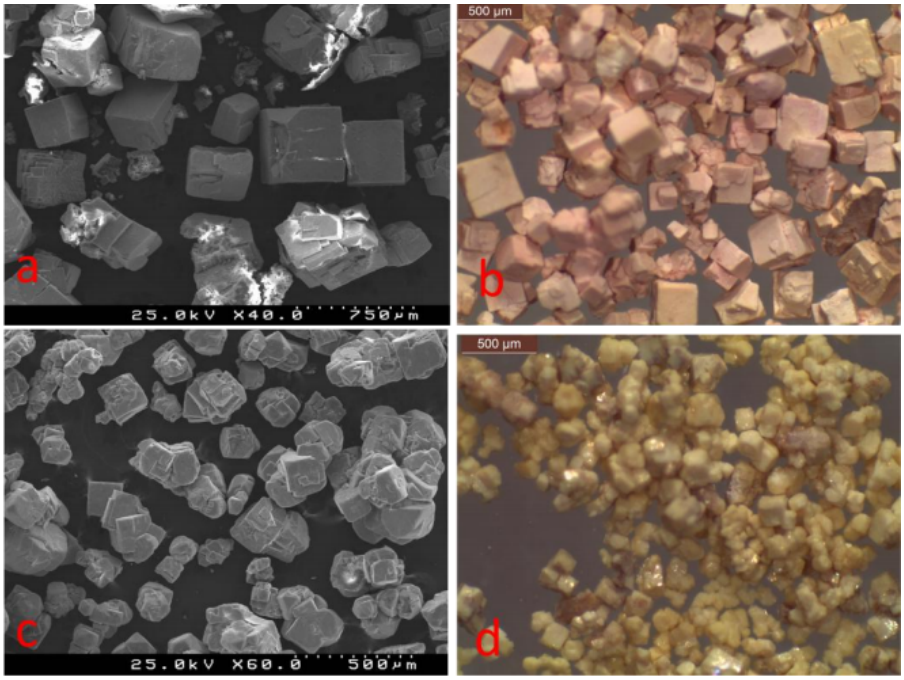

Fig. S44. SEM of: (a) Nd-IRMOF-3-CA, (c) Nd-IRMOF-3-GL, and optical microscopy photographs of (b) Nd-IRMOF-3-CA, (d) Nd-IRMOF-3-GL.

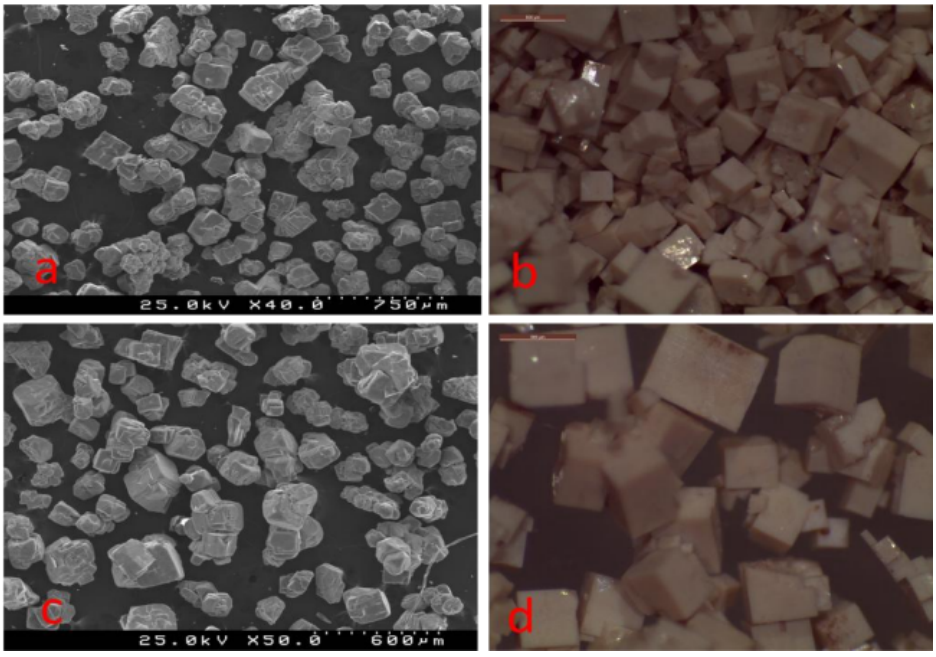

Fig. S45. SEM of: (a) Eu-IRMOF-3-CA, (c) Eu-IRMOF-3-GL, and optical microscopy photographs of (b) Eu-IRMOF-3-CA, (d) Eu-IRMOF-3-GL.

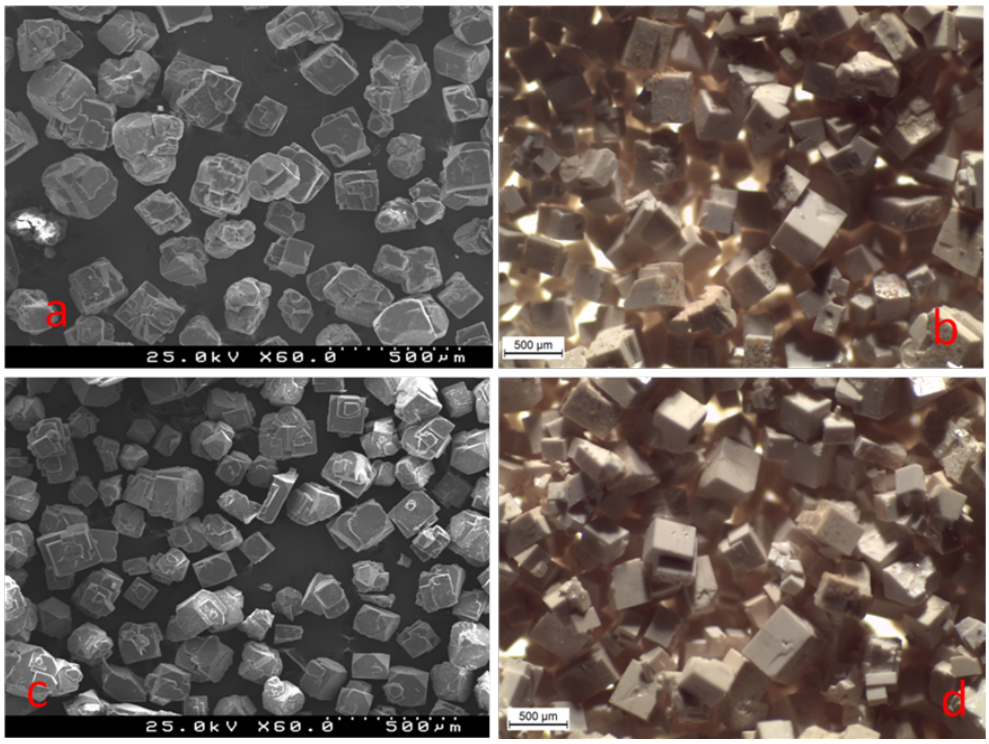

Fig. S46. SEM of: (a) Nd-IRMOF-3-MVK, (c) Nd-IRMOF-3-EM, and optical microscopy photographs of (b) Nd-IRMOF-3-MVK, (d) Nd-IRMOF-3-EM.

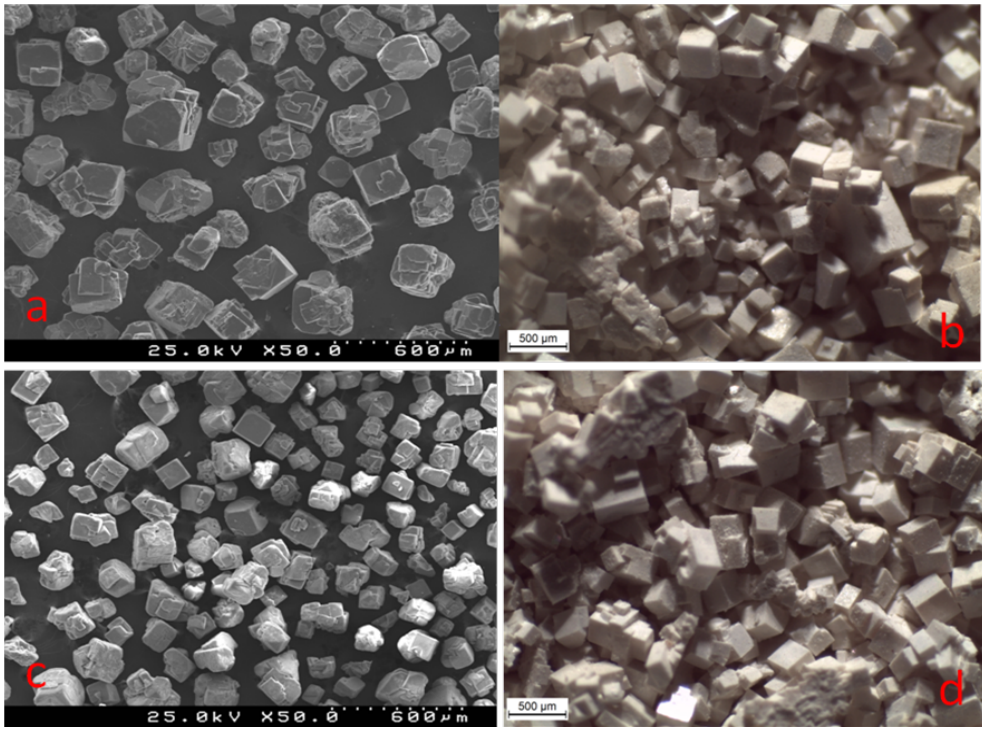

Fig. S47. SEM of: (a) Eu-IRMOF-3-MVK, (c) Eu-IRMOF-3-EM, and optical microscopy photographs of (b) Eu-IRMOF-3-MVK, (d) Eu-IRMOF-3-EM.

6. Photoluminescence spectroscopy

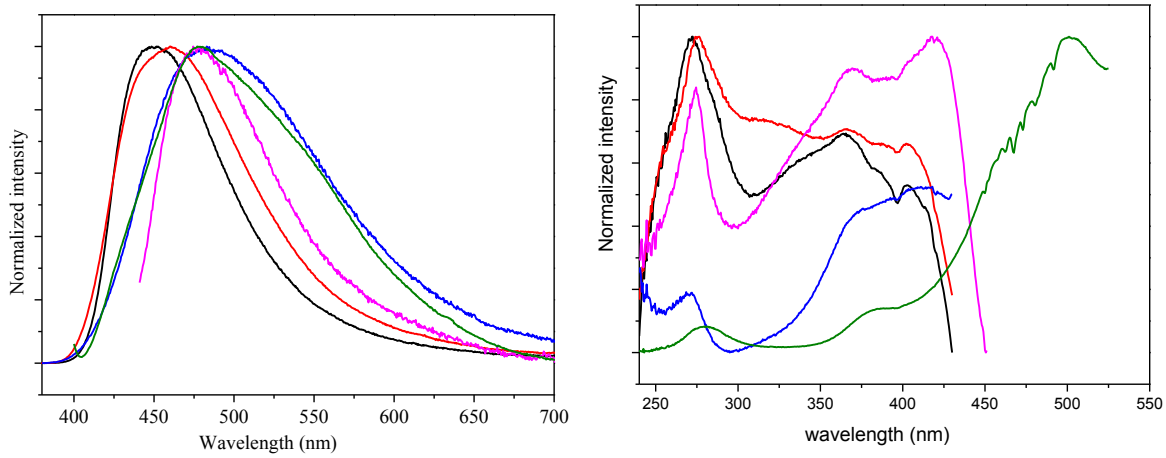

Fig. S48. Room-temperature (300 K) [left] emission spectra of IRMOF-3 (black) at 280 nm, IRMOF-3-GL (blue) at 280 nm, IRMOF-3-CA (red) at 280 nm, IRMOF-3-MVK (purple) at 421 nm and IRMOF-3-EM (green) at 385 nm; [right] excitation spectra of IRMOF-3 (black) at 450 nm, IRMOF-3-GL (blue) at 475 nm, IRMOF-3-CA (red) at 460 nm, IRMOF-3-MVK (purple) at 471 nm and IRMOF-3-EM (green) at 545 nm.

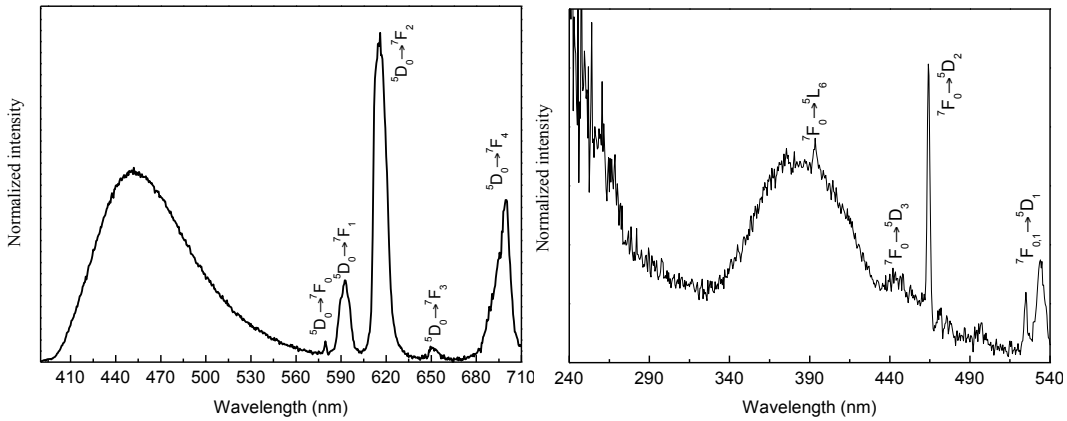

Fig. S49. Room temperature (300K) (left) emission at 370 nm and (right) excitation at 615 nm spectra of Eu-IRMOF-3-CA.

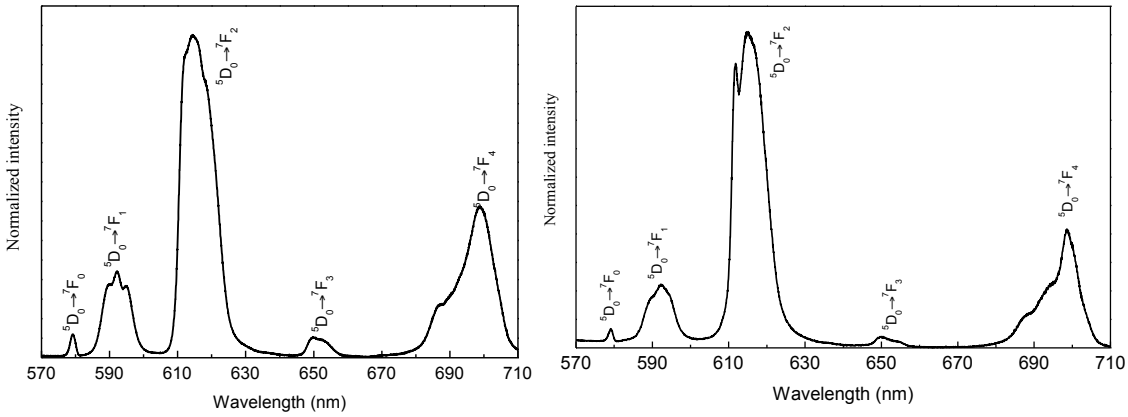

Fig.S50. High-resolution emission spectra (300K) of Eu-IRMOF-3-GL (left) excited at 430 nm and Eu-IRMOF-3-EM (right) excited at 375 nm.

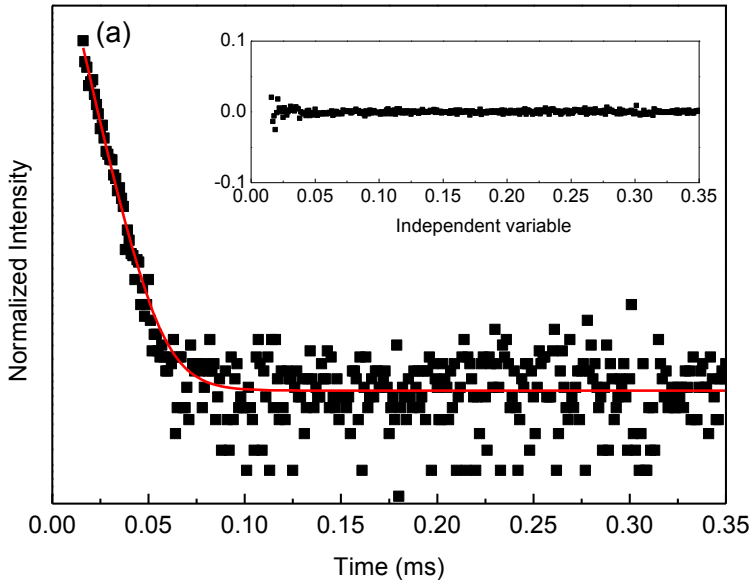

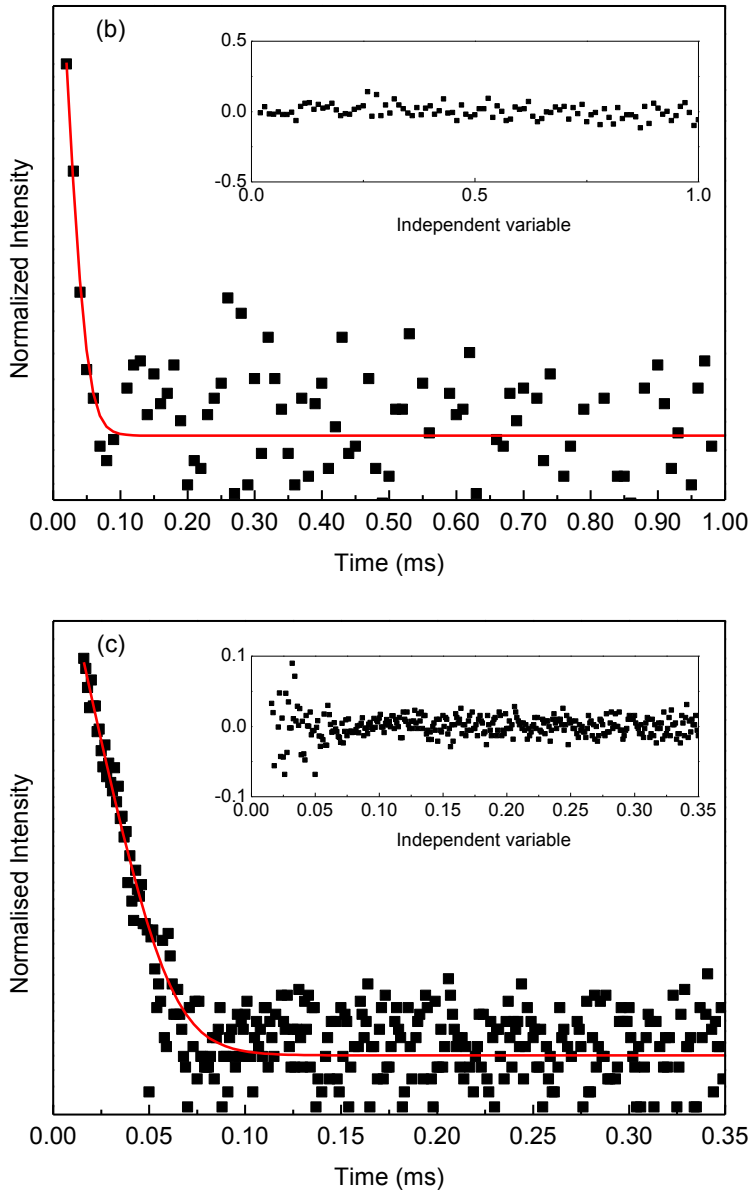

Fig. S51. Room temperature emission decay curves of (a) Nd-IRMOF-3-GL, (b) Nd-IRMOF-3-MVK and (c) Nd-IRMOF-3-CA monitored around 1064 nm and excited at (a, c) 365 nm and (b) 395 nm. The solid lines represent the data best fit ($R > 0.98$) to a single exponential function. The insets show the fit residual plot.

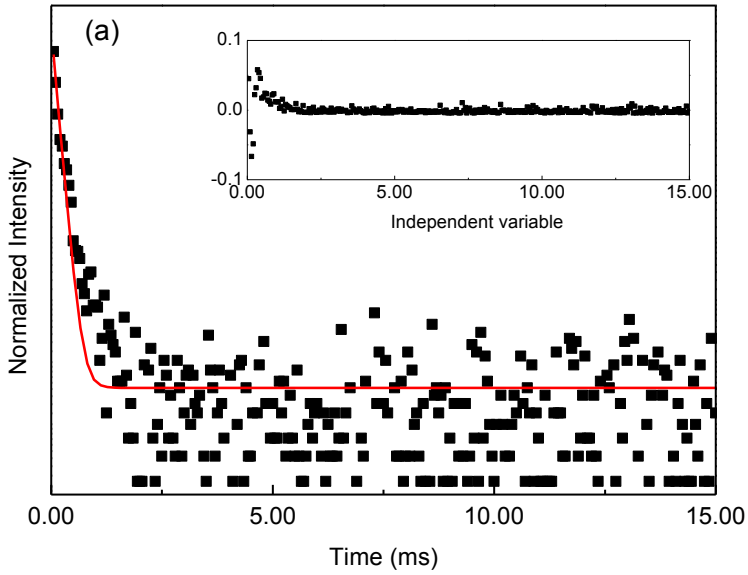
(a)
Normalized Intensity
Time (ms)
0.00
5.00
10.00
15.00
0.1
0.0
-0.1
Independent variable

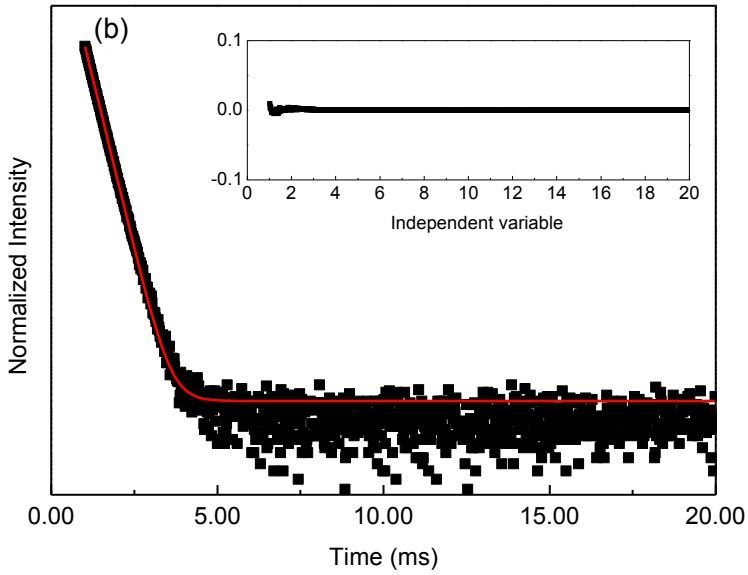
(b)
Normalized Intensity
Time (ms)
0.00
5.00
10.00
15.00
20.00
0.1
0.0
-0.1
0
2
4
6
8
10
12
14
16
18
20
Independent variable

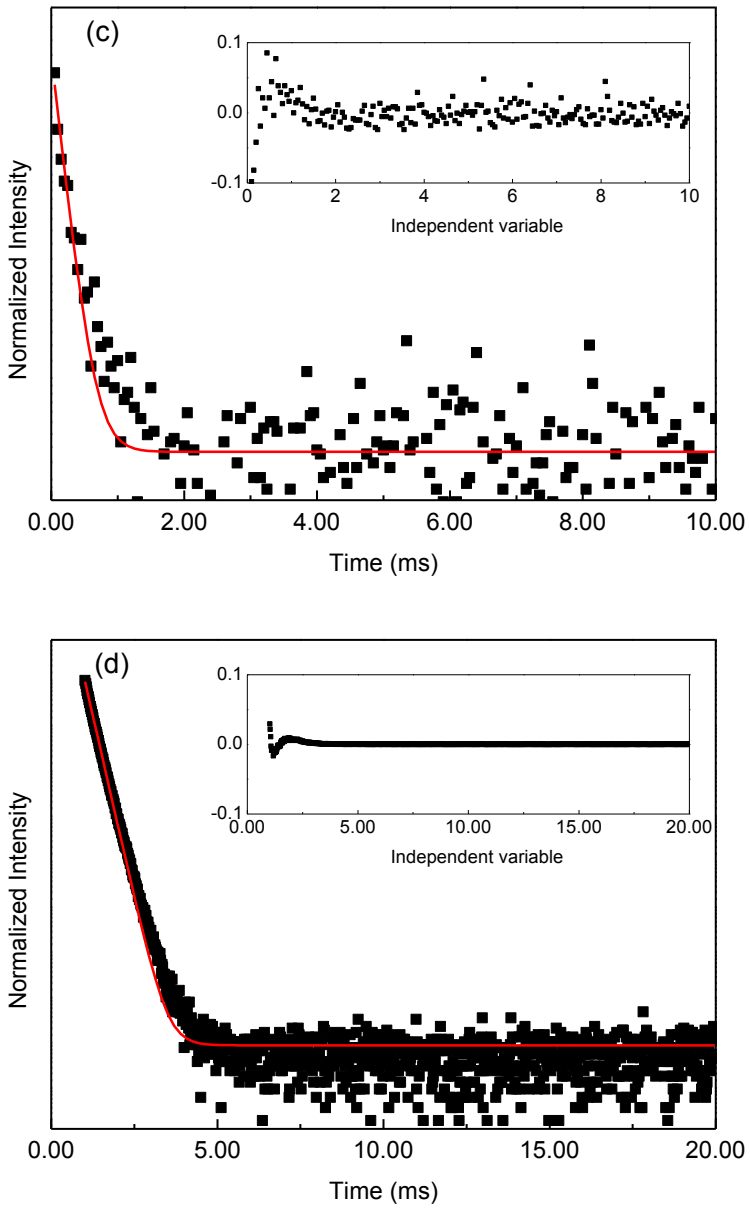

Fig. S52. Room-temperature emission decay curves of (a) Eu-IRMOF-3-GL, (b) Eu-IRMOF-3-MVK (355 nm), (b) Eu-IRMOF-3-CA and (d) Eu-IRMOF-3-EM monitored around 616 nm and excited at (a) 420 nm, (b, d) 355 nm, and (d) 380 nm. The solid lines represent the data best fit (R>0.98) to a single exponential function. The insets show the fit residual plot.